Thai, Stephen, Protein Biomarkers of Estrogenic Impact on Mouse and Rat Uterus. Masters of Science, May 2021, 69 pp., 3 tables, 4 figures, appendix, bibliography, 13 titles

Understanding the structural and morphological impact that occur in the uterus upon exposure to estrogens can reveal how these hormones elicit changes in the organ. This study seeks to revalidate the data obtained in studies of ovariectomized mice and rats treated with 17β-estradiol, followed by comparative analysis of the protein expression between the two animal models (the mice model studied by Prokai et al. [1] and the rat model presented in a dissertation by Rahlouni [2]). During these studies, female Swiss-Webster mice and Sprague-Dawley rats were ovariectomized (OVX) and divided respectively into two groups:

1) The control was treated with a corn oil vehicle while
2) The treatment group received 17β-estradiol injection for 5 days.

Raw data gathered from the earlier proteomics studies were reanalyzed using Maxquant version 1.6.17, which utilized extracted ion chromatography technique (XIC). LFQ analyst and Ingenuity Pathway Analysis (IPA) version 5.0 were used to identify proteins that were differentially regulated by 17β-estradiol and perform comparative analyses of the protein expression between OVX mice and rats. Reanalysis of OVX mice identified 59 proteins of interest at 95% confidence with 29 upregulated and 30 downregulated significantly. Reanalysis of the OVX rats identified 126 differentially expressed proteins at 95% confidence with 98 upregulated and 27 downregulated significantly. Comparative analysis using IPA® found 27 proteins unique to mice and 85 proteins unique to rats. Conversely, the OVX mice and rats shared 19 proteins regulated by 17β-estradiol in the uterus. Ingenuity Pathway Analysis® also created networks in OVX mouse and rat models showing a relationship with estrogen receptors in the nucleus, which can bind 17β-estradiol and then initiate gene transcription. Although there

is overlap between OVX mice and rat protein expression, the proteins that were found to be unique to each animal demonstrate that a complementary model using both animals provides a much broader view of uterine protein expression in OVX animals treated with 17β-estradiol. Additionally, this study illustrates the merit of reanalyzing older data with improved computational and bioinformatic tools to pinpoint proteins of interest for future analysis as potential markers of estrogenic effects in the uterus.

PROTEIN BIOMARKERS OF ESTROGENIC IMPACT

ON MOUSE AND RAT UTERUS

Stephen Thai, B.S.

APPROVED:

Laszlo Prokai, PhD, DSc (Pharmacology & Neuroscience), Major Professor

Katalin Prokai, PhD, Committee Member

Andras Lacko, PhD, Committee Member

David P. Siderovski, PhD, Chair, Department of Pharmacology & Neuroscience

J. Michael Mathis, PhD, EdD, Dean, Graduate School of Biomedical Sciences

PROTEIN BIOMARKERS OF ESTROGENIC IMPACT ON MOUSE AND RAT UTERUS

PRACTICUM REPORT

Presented to the Graduate Council of the

Graduate School of Biomedical Sciences

University of North Texas

Health Science Center at Fort Worth

in Partial Fulfillment of the Requirements

For the Degree of

MASTER OF SCIENCE

By

Stephen Duy-An Thai, B.S.

Fort Worth, Texas

May 2021

ACKNOWLEDGEMENTS

I would like to thank Dr. Laszlo Prokai for his mentorship throughout this project. His guidance has been invaluable and essential to my education over this difficult year. His understanding of the pandemic and his prioritization of my health and safety demonstrates his kind and compassionate nature. I would also like to thank members of my advisory committee, Drs. Katalin Prokai and Andras Lacko, for their support and guidance. Additional thanks to Dr. Khadiza Zaman who took time out of her busy schedule to help an inexperienced student who wanted to learn how to use different analytical programs. Her infinite patience with all of my inquiries gave me the confidence to ask even the simplest questions. I am also indebted to Stanley M. Stevens Jr, Navin Rauniyar, Vien Nguyen and Fatima Rahlouni for performing the initial studies whose data I had the privilege of reanalyzing.

I would like to thank my friends and family for supporting me emotionally and financially during this long year. I am enormously grateful to my mother and father who called me every week to provide words of encouragement and sent me care packages through the mail. Special thanks as well to my sister who takes time out of her busy life to call, check in on me, and send pictures and videos of my niece and nephew. I have grown immensely, both personally and professionally - despite of and perhaps because of - this year and for that I will always be grateful.

TABLE OF CONTENTS

Page

List of Tables

List of Figures

CHAPTER I

BACKGROUND AND LITERATURE

Proteomics

Proteomics, as defined by Kiernan, is "the use of quantitative protein-level measurements of gene expression to characterize biological process and decipher the mechanisms of gene expression control" [3]. The growth of proteomics can be traced back to large-scale nucleotide sequencing of genomic DNA, but many types of information cannot be obtained from genomics alone. Proteins responsible for the phenotype of cells and the mechanisms of disease, aging, and environmental effects would be difficult to study by using genomic data [4]. Proteomics allows for the characterization of the various protein isoforms, modifications, and potential interactions between them [5]. There are three main types of proteomics: protein expression, structural proteomics, and functional proteomics. Protein expression proteomics quantitatively measures differential protein expression between samples such as diseased and control states [6]. This can be used to identify disease-specific proteins or new proteins in cell signaling. Structural proteomics attempts to identify all proteins within a protein complex or organelle to determine their location and characterize their interactions [4]. Information gathered in this manner can help to piece together the overall structure of the cells and explain how protein expression can result in cell's unique functions or characteristics. Functional proteomics looks at a select group of proteins to study and characterize, which in turn provides information about protein signaling and disease mechanisms [4]. Mass spectrometry has emerged as one of the most accurate and

reliable methods for proteomic analyses [7]. Shotgun or gel-free proteomics is an approach used to perform identification and relative quantification of a complex protein mixture such as tissue, biological fluids, cell lysates, and extracellular proteins through techniques such as liquid chromatography (LC) coupled with mass spectrometry (MS), including tandem mass spectrometry (MS/MS) [8]. This allows investigators to perform protein identification, characterization, and relative quantification of the sample. Mass spectrometry-based methods using stable-isotope labeling have allowed for proteomic analysis, but there are limitations to this approach such as decreased experimental throughput and sensitivity from the labeling and purification steps, limited dynamic range of quantitation, compromising sample integrity due to side reactions, and a strong dependency of labeling efficiency on sample composition. Because of these limitations, label-free approaches to proteomics such as spectral counting and extracted ion chromatograms have become more productive to measure protein abundances in discovery-driven proteomics studies [9].

Label-free Quantification

In order to study differential protein expression in biological samples, rapid, reproducible, and accurate quantification is a necessity. Quantitative proteomics is composed of two major categories: label-free techniques and stable-isotope labeling. The labeling-based techniques utilized are fluorescent or isotopic reagents (e.g., isobaric tag for relative and absolute quantitation, stable isotope labeling with amino acids in cell culture, and tandem mass tagging) to differently label targets of interest. These labeling techniques are considered more accurate and reproducible, but are time-consuming and expensive to perform [10]. Label-free techniques are becoming more popular due to advancements of high-resolution LC-MS/MS instruments, as

well as reduced cost and simplified sample preparation. Two popular label-free techniques are spectral counting and extracted ion chromatograms (XICs) [9]. Spectral counting measures the number of fragmentation events (spectral counts) for all the peptides of the same protein which are summed up for the relative quantification of the protein [11]. Spectral counts can be inaccurate, as a few proteins can have a large number of counts which can lead to inaccuracies or missed proteins [12]. XICs are created by plotting the intensity of the signal observed at a chosen mass-to-charge (m/z) value or set of values in a series of mass spectra recorded as a function of retention time [13].

Targeted Proteomics

After performing proteomic discovery analysis using mass spectrometry by reviewing differentially expressed proteins in samples, it is recommended to use targeted methods for sensitive and specific protein quantification to verify target proteins of interest most often using stable-isotope (^{13}C-, ^{15}N) labeled peptides as internal standards [14]. Selected reaction monitoring (SRM) are usually done using triple quadrupole mass spectrometers and can be used on a subset of analytes which are selectively measured in predefined m/z and retention time windows [9]. SRM does have limitations, the first being low resolution quadrupole mass analyzers are not selective enough to discriminate the analytes from interferences that are commonly encountered in biological samples. Secondly, SRM is unable to monitor a large number of peptides in a single experiment [15]. Advances in instrumentation, such as the development of time-of-flight and Orbitrap mass analyzers, have allowed for the simultaneous monitoring products of a target peptide, which is called parallel reaction monitoring (PRM) that can quantify multiple peptides with increased sensitivity and specificity [16]. PRM uses targeted

MS/MS to simultaneously monitor product ions of a targeted peptide with high resolution and mass accuracy. PRM can offer higher specificity than SMR and requires less effort than traditional SRM assay [17]. A study done by Ronsien et al. comparing the linearity, dynamic range, and precision of targeted quantitative HDL proteomics of PRM and SRM found that PRM could effectively be used to quantitatively measure and verify candidate protein biomarkers in complex biological samples [18]. PRM was effectively able to rapidly quantify candidate proteins with less time and effort necessary to optimize steps required in SRM.

Hormone Therapy

Hormone therapy (HT) is used to the treat the symptoms associated with menopause, which is caused by diminished levels of sex hormones. Systemic estrogen is the most effective treatment for relief of menopausal symptoms. Unfortunately, the full benefits and risks of HT in post-menopausal women are not fully understood or defined, which is revealed by the Women's Health Initiative (WHI) clinical trials to some extent in 1998 [19]. When the results were published in 2002, the researchers had observed an increased incidence of coronary heart disease and breast cancer with a reduction of osteoporotic fractures, as a result of HT. Given these results, it appeared the risks outweighed the potential benefits which resulted in a large decrease in prescription of HT for post-menopausal women. Since that study was published, controversies about the design and conclusions from the WHI study prompted a follow up study published in 2014. This included age stratification of the cardiovascular outcomes as well as reanalysis of the WHI trials [20]. This metanalysis found that HT in younger women (50–59 years old) or early postmenopausal women (within 10 years of menopausal onset) had a beneficial effect on the cardiovascular system. Increased risks of breast and endometrial cancer, two of the most

prevalent cancers in the US, are associated with HT usage [21-23]. Various studies have been done showing increased risk of endometrial cancer with estrogen use in menopausal women who have not had a hysterectomy [22, 24]. With the new changes and findings of the risks and benefits associated with HT, further studies, such as characterization of protein changes, would benefit the understanding of HT's impact to better elucidate the underlying mechanisms associated with cancer and the biological effects of HT.

Endometrial Cancer

Endometrial cancer is the fourth most common cancer among women in the US with approximately 47,000 cases diagnosed each year [25]. As the leading gynecological malignancy in the Western world, early diagnosis is key to improving survival. When diagnosed at an early stage, endometrial cancer is highly curable and has excellent overall 5-year survival rates [26]. Endometrial cancer has historically been classified in two histological categories by Bokhman's dualistic model of endometrial cancer: type 1 (70%) and type 2 (30%) [27]. Type 1 is associated with obesity, hyperlipidemia, diabetes and is caused by hypoestrogenism due to anovulatory uterine bleeding, infertility or late onset of the menopause, but has a positive prognosis. Additionally, Type I is associated with hormone receptor positivity and maybe be preceded by a precancerous condition (atypical hyperplasia). Type II tumors are estrogen independent, high grade and clinically aggressive. Biological specimens that are used to investigate endometrial cancer include serum/plasma, hysterectomy specimens, uterine aspirates/tissue biopsies, uterine lavage samples, and urine [28]. Because endometrial cancer is linked in part to continuous estrogenic stimulation of the uterus by HT, understanding of the hormone's impact on the organ in an animal model is a critical component of the research for a cure. However, estrogen's effect

on systems level has been poorly understood even in these experimental paradigms. The study by Prokai et al. [1] has addressed the latter for the first-time using proteomics as enabling methodology and relying on 17β-estradiol (E2) as an estrogen.

Mouse versus Rat Models

As in all models used in science, there are advantages and disadvantages of using various models. Mice and rats are two of the most common animal models used in biomedical experiments [29]. Mouse models became increasing popular in the 1970s and have only grown due to the volume of techniques available to genetically manipulate mice. Genomic data for rats has been slow to catch up, but are now available for this animal as well [30]. As both models have similar technologies to manipulate mice and rats, scientists are able to choose the most appropriate model based upon biology and area of research. Obviously, rats are not just large mice and differ in their suitability to be used in biomedical research. Due to their larger size, rats are preferred model for research requiring surgical procedures, serial blood draws, and physiological measurements. Additionally, rats are more commonly used to model behavioral studies as they are more social than mice and their behavior more closely mimics that of humans [31]. The smaller size of the mouse is advantageous in optogenetics, which is a technique for the precise stimulation or inhibition of neuronal pathways [29]. In a study done by Lemini et al., ovariectomized mice and rats were compared to understand how lack of endogenous ovarian estrogen affects hemostatic coagulation markers [32]. This study found that, in general, the hemostatic parameters of OVX mice changed in greater magnitude and did not return to baseline values, while those in OVX rats did. Additionally, it described a critical surgery recovery period of about one week for OVX animals to minimize hematological changes which could impact

experimental results. Of note, the “gold standard” for estrogenic effects in the uterus is an in vivo uterotrophic bioassay in rats [33], and mice are not utilized commonly for this purpose. Further comparative studies between mice and rats demonstrate how experimental treatment may affect the animals, but also increase understanding in the methods that might result in the most optimal results for each model.

CHAPTER II

RESEARCH PROJECT

Specific Aims

In the initial research proposal, our goal was to provide verification of label-free proteomics results involving OVX mice treated with E2 as previously performed by Prokai et al. [1] and further the study by performing targeted proteomic analyses of two proteins of interest, lumican (LUM) and transglutaminase 2 (TGM2) utilizing parallel reaction monitoring. However, due to weather delays and other unforeseen circumstances, we were required to pivot our study. In this revised study, we aim to reanalyze and compare protein expression data of OVX rats and mice previously performed by Prokai et al. [1] and a study performed by Rahlouni (author) and Prokai (advisor) [2]. Originally analyzed using spectral counting, MaxQuant and LFQ analyst will reanalyze the data using XICs to provide verification of results and further insight into estrogen's uterothrophic effect in both animal models. Furthermore, this study will use Ingenuity Pathway Analysis® to explore differences and similarities in protein expression in OVC mice and rats to further understand E2 uterotrophic effects.

Significance

Hormone therapy can be used to treat the symptoms associated with menopause, but has risks such as increased incidence of blood clot, stroke, and breast/endometrial cancer. Studying changes in protein expression that occur in the uterus could help further our understanding about the differential protein expression that occurs when taking estrogen. Endometrial cancer is the most common female reproductive organ cancer, but when diagnosed early has excellent

survival rates. Understanding the protein changes occurring in the uterus when females undergo hormone replacement therapy could provide insight into potential protein biomarkers for endometrial cancer, as well as improve early detection. The proposed study is significant because it will continue to examine the differential protein expression previously performed in mice and utilize newer and quantitatively more accurate analytical approaches to enhance upon the findings of previous studies. It will also strive to rigorously validate the changes that are occurring in protein levels in the uterus and potentially unlock novel biomarkers for endometrial cancer linked to persistent estrogenic stimulation of the tissue. Additionally, comparative analysis of the OVX mice and rat models will help to provide further insight into the different proteomic changes that are occurring in the two models and provide more evidence of potential biomarker proteins for targeted proteomic techniques and future analysis.

Materials and Methods

Description of the parent study as performed in Rapid Label-free Identification of Estrogen-induced Differential Protein Expression In Vivo from Mouse Brain and Uterine Tissue by Prokai et al. [1]

Animal Model

Swiss-Webster mice were used for all experiments. All mice were maintained in an animal care facility in accordance with institutional guidelines and those set by the Declaration of Helsinki and the Guiding Principles in the Care and Use of Animals (DHEW Publication, NIH 80-23) as approved by the Institutional Animal Care and Use Committee at the University of North Texas Health Science Center. Ovariectomy of the mice (8 animals divided into two

groups) was done one week prior to shipping by their supplier (Charles River Laboratories, Wilmington, MA) then allowed to adapt in the animal facility of the University of North Texas Health Science Center for approximately two weeks before starting daily injections with vehicle (corn oil, 60 µl per injection) control or E2 (50 µg/kg body weight in corn oil vehicle) for 5 consecutive days between 10:00 a.m. and 12:00 a.m. The mice were sacrificed by cervical dislocation and an abdominal incision was made and the uterus removed by cutting at the junction of the uterus and vagina at the site of ovariectomy on each horn. Uterus samples had excess fat and connective tissue removed prior to the organs being blotted and weighed. All tissue samples were stored at -80 °C until analysis.

Sample Preparation

The tissue samples were prepared following the procedure of Shi et al [34]. Carbamindomethylation of thiol groups was performed by adding 5 mM iodoacetamide and incubating for 30 min in the dark at room temperature before a 4-fold dilution with 50 mM ammonium bicarbonate. The samples were then incubated overnight at 37 °C with 1 µg of sequencing grade trypsin (Promega, Madison, WI) which was subsequently quenched using 1 µL of acetic acid.

Discovery-Driven Proteomics by LC-MS/MS Analysis

The samples were analyzed using a hybrid linear ion trap (LTQ)-Fourier transform ion cyclotron resonance (FTICR, 7 T) mass spectrometer (LTQ-FT, Thermo, San Jose, CA) equipped with a nanoelectrospray ionization source and operated with Xcalibur (version 2.2) data acquisition software. Protein digests were loaded onto a PepMap C18 capillary trap (LC

Packings, Bannockburn, IL) and desalted with 3% acetonitrile, 1% acetic acid for 5 min prior to injection onto a 75 µm i.d. x 10 cm long PicoFrit C18 analytical column (New Objective, Woburn, MA). Following a peptide desalting and injection onto the analytical column, a linear gradient provided by a NanoLC-2D (Eksigent) was carried out to 40% acetonitrile in 60-120 min at 250 nL/min. The data-dependent mode of acquisition was utilized in which an accurate m/z survey scan is performed in the FTICR cell followed by parallel MS/MS linear ion trap analysis of the top five most intense precursor ions. FTICR full-scan mass spectra were acquired at 100000 mass resolving power (m/z 400) from m/z 350 to 1500 using the automatic gain control mode of ion trapping. CID in the linear ion trap was performed using a 3.0-Th isolation width and 35% normalized collision energy with helium as the target gas. The precursor ion that had been selected for CID was dynamically excluded from further MS/MS analysis for 60 s.

Data Analysis

MS/MS data generated by data dependent acquisition via the LTQ-FT were extracted by BioWorks version 3.3 (Thermo) and searched against a composite IPI mouse protein sequence database containing both forward and randomized sequences (version 3.35, number of entries were 51490 x 2) using the Mascot search algorithm (version 2.2, Matrix Science, Boston, MA). Of note, the international protein index (IPI) is now a defunct protein database launched in 2001 and closed in 2011 by the European Bioinformatics Institute.

The software program Scaffold (version 2.0, Proteome Software Inc., Portland, OR) was employed to validate MS/MS-based peptide and protein identifications, as well as to obtain spectral counts as measures of protein abundance. A likelihood ratio test for independence (G-test) was then utilized to determine statistical significance for each protein ratio. Ratios were

considered significant at $p<0.05$. Bioinformatics included Cytoscape 2.6.0 equipped with the BiNGO 2.0 plug-in (http://www.psb.ugent.be/cbd/papers/BiNGO/) to determine over- or under-represented gene ontology (GO) categories. Ingenuity Pathway Analysis® (IPA, version 5.0, Ingenuity Systems, Redwood City, CA) was also utilized to determine biological processes represented by the proteins up- and down-regulated in the mouse uterus by E2 treatment.

Description of the parent study as performed in the thesis work entitled Quantitative Proteomic Investigation of Estrogenic Endocrine-Disrupting Effects in the Rat Uterus by Rahlouni (author) and Prokai (advisor) [2].

Animal Model

Sprague Dawley rats were used for all experiments. All rats were maintained in an animal care facility in accordance with institutional guidelines which was conducted in accordance with guidelines set for in the Declaration of Helsinki and the Guiding Principles in the Care and Use of Animals (DHEW Publication, NIH 80-23) as approved by the Institutional Animal Care and Use Committee at the University of North Texas Health Science Center. Ovariectomy of the rats (8 animals divided into two groups) was done one week prior to shipping by their supplier (Charles River Laboratories, Wilmington, MA) then allowed to adapt in the animal facility of the University of North Texas Health Science Center for approximately two weeks before starting daily injections with vehicle (corn oil, 60 µl per injection) control or E2 (50 µg/kg body weight in corn oil vehicle) for 5 consecutive days between 10:00 a.m. and 12:00 a.m. The rats were sacrificed by cervical dislocation and an abdominal incision was made and the uterus removed by cutting at the junction of the uterus and vagina at the site of ovariectomy

on each horn. Uterus samples had excess fat and connective tissue removed prior to the organs being blotted and weighed. All tissue samples were stored at -80 °C until analysis.

Sample preparation

Approximately one-tenth of the whole uterus (10 mg control and 50 mg E2-treated) was incubated in 200 µL of 8M urea for 30 minutes. The samples were centrifuged for 5 minutes at 1400x g and the supernatant was collected. Protein content of uterine extracts was determined by a microBCA assay (Bio-RAD, CA). Approximately 100 µg of protein from each sample was used for further processing. Samples were reduced with 1 mM dithiothreitol (DTT) for 30 min at 65°C to reduce the disulfide bonds. Carbamidomethylation of the thiol groups was performed by the addition of 5 mM iodoacetamide (IAA) and incubation for 30 min at room temperature in the dark. Excess IAA was quenched by the addition of DTT for 5 min.

Data-Dependent LC-MS/MS Data Acquisition for Discover-Driven Shotgun Proteomics

The samples were analyzed in triplicate using a hybrid linear ion trap−Fourier transform ion cyclotron resonance (7-T) mass spectrometer (LTQ-FT, Thermo Scientific) equipped with a nano-electrospray ionization (ESI) source and operated with Xcalibur (version 2.2) and LTQ Tune Plus (version 2.2) data acquisition software. Online reversed-phase high performance liquid chromatography (RP-HPLC) was performed with an Eksigent nano-LC-2D (Eksigent, Dublin, CA) system. An amount of 5 µL of the sample was automatically loaded onto the IntegraFrit™ sample trap (2.5 cm x 75 µm) (New Objective, Woburn, MA), for sample concentration and desalting, at a flow rate of 1.5 µl/min in a loading solvent containing 0.1% (v/v) acetic acid and 5% (v/v) acetonitrile in 94.9% (v/v) water prior to injection onto a reverse phase column (NAN75-15-03-C18-PM; 75 µm i.d. x 15 cm, LC Packings, Sunnyvale, CA)

packed with C18 beads (3 µm, 100 Å pore size, PepMap). Mobile-phase buffer A consisted of 0.1% (v/v) acetic acid and 99.9% (v/v) water, and mobile-phase buffer B consisted of 0.1% (v/v) acetic acid and 99.9% (v/v) acetonitrile. Following desalting and injection onto the analytical column, peptides were separated using the following gradient conditions: (1) 5 min in 95% solvent A for equilibration; (2) linear gradient to 40% solvent B over 90 min and holding at 40% solvent B for isocratic elution for 5 min; (3) increasing the gradient to 90% solvent B and maintaining for 5 min; and finally (4) 95% solvent A in the next 20 min. The flow rate through the column was 250 nL/min. Peptides eluted through a Picotip emitter (internal diameter 10 ± 1 µm; New Objective, Woburn, MA) and were directly sampled by the nano-electrospray source of the mass spectrometer. Spray voltage and capillary temperature during the gradient run were maintained at 2.0 kV and 250 ºC. Conventional data-dependent mode of acquisition was utilized in which an accurate m/z survey scan was performed in the FTICR cell followed by parallel MS/MS linear ion trap analysis of the top five most intense precursor ions. FTICR full-scan mass spectra were acquired at 50000 mass resolving power (m/z 400) from m/z 350 to 1500 using the automatic gain control mode of ion trapping. Peptide fragmentation was performed by collision induced dissociation (CID) in the linear ion trap using a 3.0-Th isolation width and 35% normalized collision energy with helium as the target gas. The precursor ion that had been selected for CID was dynamically excluded from further MS/MS analysis for 60 s.

Database Search, Label-Free Relative Quantification, and Pathway Analysis

MS/MS spectra were searched against the UniProt protein sequence database (species:Rattus norvegicus, 29,938 entries) using the Mascot search engine (version 2.2; Matrix Science, Boston, MA, USA) run from Proteome Discoverer (version 2.3; Thermo

FisherScientific). A parent ion mass tolerance and fragment ion mass tolerance were set to 25 ppm and 0.80 Da, respectively, allowing only one missed cleavage in our search filters and limiting FDR to 0.01 (1%). Cysteine carbamidomethylation was indicated as fixed modification and methionine oxidation was designated as variable modification. They used Scaffold software (version 4.3.0, Proteome Software Inc.; Portland, OR, USA) to validate our search results using the Peptide Prophet and Protein Prophet algorithms requiring over 95% by Peptide Prophet Algorithm and 99% probabilities if protein identifications were assigned, respectively, and contained at least two identified unique peptides for each protein. Scaffold 4 was used to extract the MS-based peptide precursor ion abundance for each identified peptide and calculated the total precursor intensity for each protein. A student's t-test was performed on the normalized precursor intensity values and accepted at $p<0.05$ and required at least a 1.5-fold change for significance. Ingenuity Pathway Analysis® (IPA®, Qiagen, Redwood City, CA) was utilized to derive annotations along with potential protein interaction networks from the associated proteins in the rat uterus.

Reanalyses

Verification of the results of Prokai et al. [1] and Rahlouni [2] was done by reanalysis of their dataset using MaxQuant (version 1.6.17.0) and by searching protein sequences of the Uniprot mouse and rat protein database (available at https://www.uniprot.org/ with version released on July 3, 2020, including 55466 entries under Proteome ID of UP000000589 (mouse) and 21588 entries under Proteome ID of UP000002494 (rat)). The criterion of $\leq$0.01% protein false discovery rate (FDR) was applied to the search conducted with default parameters and selecting label-free quantification (LFQ) of the program as an option. MaxQuant's LFQ utilizes

XIC technique for relative protein quantification from the total intensity of peptide ions distinguished by their m/z. LFQ-Analyst was used to identify differentially regulated proteins and generate box plots of proteins significantly regulated by E2. To obtain differentially expressed proteins, p-value and log2 fold change cutoffs were set to 0.05 and 1.0, respectively, with FDR correction based on the Benjamini-Hochberg procedure. IPA® was used to determine the over- and under-represented biological processes from the proteome dataset relying on the results of LFQ-Analyst, along with determining canonical pathways and assembling interaction networks driving the uterotrophic effects of E2 in the mouse uterus. These pathways were accepted at the significance level of $p<0.05$.

Results

Upon reanalysis of the study performed by Prokai et al. [1], MaxQuant and LFQ analyst identified 59 differentially regulated proteins at a 95% confidence interval with 29 upregulated and 30 downregulated significantly (Table S1 and S2). Reanalysis of the rat study performed by Rahlouni [2] identified 126 differentially expressed proteins between OVX rats treated with E2 at 95% confidence interval with 98 upregulated and 28 downregulated (Table S3 and S4). Volcano plots generated using LFQ analyst of both OVX mice and rats showed the differences in protein expression for all proteins, along with protein plots of TGM2 and LUM (Figure S1 and S2).

Comparative IPA® analysis of E2-regulated proteins found 27 proteins unique to mice, 85 unique to rats, and 19 proteins shared between mice and rats (Table 1, 2 and 3). Proteins found to be significantly affected by E2 in the OVX mouse and rat uteri were mapped to 4 and 7 networks, respectively (Table S5, Figure S3-S11). Associated functions in the network for the

mice included: metabolic disease, neurological disease, protein synthesis, cancer, gastrointestinal disease, infectious disease, drug metabolism, endocrine system disorders, glutathione depletion in the liver, development disorder, hematological disease, and organismal injury and abnormalities. Associated functions in the network for rats included: cell morphology, cellular assembly and organization, cellular function and maintenance, drug metabolism, free radical scavenging, small molecule biochemistry, cancer, gastrointestinal disease, hepatic system disease, humoral immune response, neurological disease, organismal injury and abnormalities, cancer, gastrointestinal disease, hepatic system disease, cell-to-cell signaling and interaction, molecular transport, small molecule biochemistry, developmental disorder, ophthalmic disease, and organismal injury and abnormalities. Network 6 for OVX rats and network 4 for OVX mice treated with E2 displayed relevance to estrogen biology, which was shown by the presence of an estrogen receptor (ER) as a node in two specific networks (Figures 1 and 2). IPA® was also used to generate lists of the canonical pathways, physiological system development and function, and diseases and disorders shared and different between OVX rats and mice treated with E2 (Table S6-S8). The comparative analyses of the canonical pathways and diseases and biological functions were summarized as heatmaps (Figures 3 and 4).

Discussion

In this study, we sought to reanalyze data previously obtain in ovariectomized mice and rats using MaxQuant, LFQ analyst, and Ingenuity Pathways Analysis® to provide validation of the protein expression using XICs for the entire proteomic data set. For the mouse study performed by Prokai at al. [1] and the rat study performed by Rahlouni [2], MaxQuant proved to be a powerful analytical tool in validating the data that had previously been obtained. The

number of significant proteins identified initially by Prokai et al. and upon reanalysis differed greatly. Spectral counting utilizes the number of spectra matched to peptides from a protein as a surrogate measure of protein abundance. This technique is capable of providing estimates about the changes in proteomic abundances, but is considered not as quantitatively accurate in comparison to other quantitative proteomic techniques [35]. XICs are created by plotting the intensity of the signal observed at a chosen m/z value in a series of mass spectra recorded as a function of retention time. Although MaxQuant is capable of performing XIC analysis on proteomic data sets, it can be less accurate than other, namely non-free, programs. A study done by Smith and Tostengard compared MaxQuant to other popular algorithms used for XIC extraction such as Massifquant, MatchedFilter, CenWave, and MZMine2 and showed that MaxQuant did not recover many of the XICs with the highest intensities, and performance was unpredictable on the dataset used and was not similar to other algorithms' performance [36]. Despite these flaws, the benefit of MaxQuant is that no payment or licensing is required, it is also being updated regularly, and improvements are being made to its XIC algorithm to help increase its accuracy and precision in protein identification. Thus, it remains a powerful tool for XIC analysis of MS/MS data.

IPA® networks generated for both OVX mice and rats confirm the role of protein expression changes through E2's interaction of an estrogen receptor. The network of the mice reflected the target genes of the hormone, while the network for the rat study highlighted estrogen receptor-mediated signaling. Many of these protein interactions in the network generated by IPA® are at play both directly and indirectly. The heatmaps generated using IPA® also highlighted the differences between the OVX mice and rat models, showing little overlap in

canonical pathways outside of LXR/RXR activation. The heatmaps of diseases and biological functions of the OVX mice and rats did reveal more overlap between the two models.

The comparative analysis of OVX treated mice and rats treated with E2 provides insight into the strengths and weaknesses of the different animal models. As a basic technical consideration, rats are larger and heavier than mice, which has advantages in surgical procedures, blood pressure monitoring, and neurocognitive exercises. Mice have been found to be an important model for certain hereditary diseases and optogenetics. In this study primarily focused on the protein expression in the uterus comparatively between mice and rats, we found that rats had almost 100 more proteins that were covered by proteomic analyses using the same instrument and methodology, which could allow for a broader analysis of the expression changes that are occurring with E2 treatment. A previous study done by Lemini et al. explored changes occurring in OVX mice and rats, but was focused on the hemostatic markers [32]. Otherwise, to date, we have found no other studies on the comparison of the effects of E2 on ovariectomized rats and mice. This comparative analysis of mice and rats is particularly advantageous as the protocol used to treat and care for the animals was identical and performed in the same lab leaving only human error as the difference between treatment of the two animals. With the identical quantitative analysis between the two animal models, less concern can be placed upon differences in protocol and focus can instead be shifted to highlight differences and similarities between the two animal models.

This comparative analysis of the differences in protein expression upon E2 treatment between OVX rats and mice may also offer insight into potential biomarkers for endometrial cancer. The common proteins found between rats and mice could provide a framework for targeted proteomic analysis. Specifically, TGM2 and LUM could be further evaluated using

targeted proteomics to provide quantitative changes occurring with E2 treatment. TGM2 has been reported to be involved in a variety of cellular functions, many of which result in tumor cell proliferation, survival, and metastatic spread [37]. TGM2 has also been reported as both a potential tumor suppressor and promoting factor, and its role as an enzyme in cancer requires further investigation. TGM2 has not been previously identified as estrogen-regulated and a further targeted proteomic study using a similar OVX rodent model could provide additional insight into E2's effect on the enzyme. LUM is a small leucine-rich repeat proteoglycan and a component of the extracellular matrix; therefore, it can act as a regulator for cell proliferation, gene expression, and wound healing. A study done by Ishiwata et al. reported a potential correlation between LUM expression in stromal tissues and female hormones [38]. Findings of LUM expression changes in both OVX mice and rats treated with E2 warrants further investigation of the potential of LUM as a biomarker for structural changes that may be occurring. Recently in a new study done by Prokai et al. [39] building upon the study done by Rahlouni [2] using LTQ Orbitrap Velos Pro (a faster and more sensitive instrument), 165 E2-regulated proteins of interest were identified via spectral counting. Of those proteins, 143 were upregulated and 22 were downregulated. Follow-up targeted proteomics on TGM2, eukaryotic translation elongation factor 2 (EEF2), selenium binding protein 1 (SELENBP1), and LUM using heavy-isotope labeled peptide standards was also performed. In addition, this study included bisphenol A (BPA), a well-known example of estrogenic endocrine disrupting chemical, in a comparative analysis with E2 treatment.

Summary and Conclusions

This study validates the results from the prior studies performed by Prokai et al. [1] and Rahlouni [2] on both OVX mice and rats. The use of XICs also expanded results that had

initially been obtained using spectral counting. IPA® networks confirm that protein expression changes occur mainly through E2's interaction with the estrogen receptors. However, the network from the mouse study reflected the target genes of the hormone, while the network from the rat study highlighted estrogen receptor-mediated signaling. In addition, many other protein-protein interactions are also at play both directly and indirectly. Overall, results from the two rodent models can be considered complementary. Understanding that each model has its advantages and disadvantages can contribute to a broader picture of the protein expression occurring in the uteri of OVX mice and rats treated with E2. Through comparative analysis, proteins unique to OVX E2-treated mice and rats were identified, which demonstrated that a complementary model of both mice and rats could assist in identifying a fuller protein complement in a study. Both models have their advantages and disadvantages. However, mice and rat models together can help to build a more complete understanding of protein expression changes in a study focusing on the impact of the hormone. Further experiments targeting TGM2 and LUM could advance focus on potential biomarker discovery for uterotrophic effects that are occurring with hormone therapy.

Table 1. Comparative analysis by IPA® of E2-regulated proteins in the uterus unique to the OVX mice. There were 27 proteins found to be unique to OVX mice compared to rats; 8 proteins with the largest fold change for control versus E2-treated (negative log fold change), and 8 proteins with the largest fold change for E2-treated versus control (positive log fold change), respectively, shown here as examples. Gene ID can be found using Ensembl, Entrez Gene, GeneBank, or GenPept.

Protein Name	Gene ID	Log Fold Change	p-value
Caveolae associated protein 1	O54724	-3.45	1.81E-08
Glutathione S-transferase mu 5	P10649	-2.91	3.99E-10
Triosephosphate isomerase 1	P17751	-2.79	0.0106
Annexin A6	P14824	-2.34	0.000000688
Malate dehydrogenase 1	P14152	-2.31	0.000000345
PDZ and LIM domain 3	O70209	-2.29	0.000103
Vinculin	Q64727	-2.09	0.0000256
Peroxiredoxin 6	O08709	-1.94	0.0065
Hemopexin	Q91X72	1.98	0.0081
Apolipoprotein A2	P09813	2.1	0.000595
Serpin family A member 3	P07759	2.28	0.00744
H2A clustered histone 14	Q8CGP5	3.04	0.00000856
Filamin A	Q8BTM8	3.2	0.00000106
Myosin heavy chain 11	A0A2R8VHF9	3.21	6.24E-09
Apolipoprotein A1	Q00623	3.42	0.000802
Eukaryotic translation elongation factor 1 alpha 1	P10126	3.75	0.00000474

Table 2. Comparative analysis by IPA® of E2-regulated proteins in the uterus unique to the OVX rats. There were 85 proteins found to be unique to OVX rats compared to mice; 8 proteins with the largest fold change for control versus E2-treated (negative log fold change), and 8 proteins with the largest fold change for E2-treated versus control (positive log fold change), respectively, shown here as examples. Gene ID can be found using GenPept, UniProt, or Swiss Prot.

Protein Names	Gene ID	Log Fold Change	p-value
Selenium binding protein 1	Q8VIF7	-3.63	7.23E-09
C-reactive protein	P48199	-3.58	4.81E-09
BAF nuclear assembly factor 1	Q9R1T1	-3.52	0.000325
Heparin binding growth factor	Q8VHK7	-3.49	0.0000368
Retinol binding protein 1	P02696	-2.82	0.000015
Dipeptidyl peptidase 7	Q9EPB1	-2.65	4.39E-08
Hemoglobin subunit beta	A0A0G2JTW9	-2.62	0.00248
Melanoma cell adhesion molecule	Q9EpF2-2	-2.52	0.000489
S100 calcium binding protein A6	P05964	3.24	0.0000229
Valosin containing protein	P46462	3.26	7.79E-09
Keratin 7	G3V712	3.28	5.68E-09
Phosphoglycerate kinase 1	P16617	3.36	0.00000398
Keratin 8	Q10758	3.51	2.68E-08
Keratin 19	Q63279	4.67	2.23E-11
S100 calcium binding protein G	P02634	5.82	1.49E-13
Lactate dehydrogenase A	P04642	5.87	6.97E-09

Table 3. Comparative analysis by IPA® of the 19 E2-regulated uterus proteins shared between the OVX mice and rats. Gene ID can be found using GenPept, UniProt, or Swiss Prot.

Protein Names	Gene ID	Rats		Mice	
		Log Fold Change	P-value	Log Fold Change	P-value
ATP synthase F1 subunit alpha	P15999	2.7	7.06E-07	1.69	9.97E-03
Complement C3	M0RBF1	2.55	6.89E-04	2.74	1.12E-05
Carbonic anhydrase 2	P27139	-2.6	9.23E-04	1.72	6.67E-04
Desmin	Q6P725	2.07	2.49E-05	2.74	5.42E-05
Eukaryotic translation elongation factor 2	P05197	3.87	4.56E-09	1.58	9.47E-04
Eukaryotic translation elongation factor 1 alpha 1	P62630	5.25	5.05E-07	3.75	4.74E-06
Glutathione S-transferase pi 1	P04906	-1.77	0.0329	-2.38	6.34E-06
Heat shock protein 90 beta family member 1	Q66HD0	2.85	7.16E-06	2.1	5.72E-05
Heat shock protein family A (HSP70) member 5	P06761	1.69	1.66E-03	2.86	1.19E-06
Lamin A/C	G3V8L3	2.45	5.49E-07	-2.11	1.76E-08
Lamin B1	P70615	-1.56	0.0106	-2.99	4.09E-08
Lumican	P51886	-2.07	8.8E-08	-1.57	3.36E-03
Protein disulfide isomerase Family A member 6	Q63081	1.79	3.02E-03	1.45	0.0136

Phosphatidylethanolamine Binding protein 1	P31044	1.79	3.02E-03	1.45	0.0136
Pyruvate kinase M1/2	P119802	3.61	4.42E-06	2.45	7.44E-06
Proline and arginine rich end leucine rich repeat protein	Q9EQP5	2	7.79E-04	-2.89	1.39E-07
Serpin family H member 1	Q5RJR9	3.45	2.97E-09	2.29	0.0012
Superoxide dismutase 1	P07632	-1.57	6.57E-07	-2.76	4.65E-06
Transglutaminase 2	Q9WVJ6	4.79	1.91E-11	1.99	1.43E-03

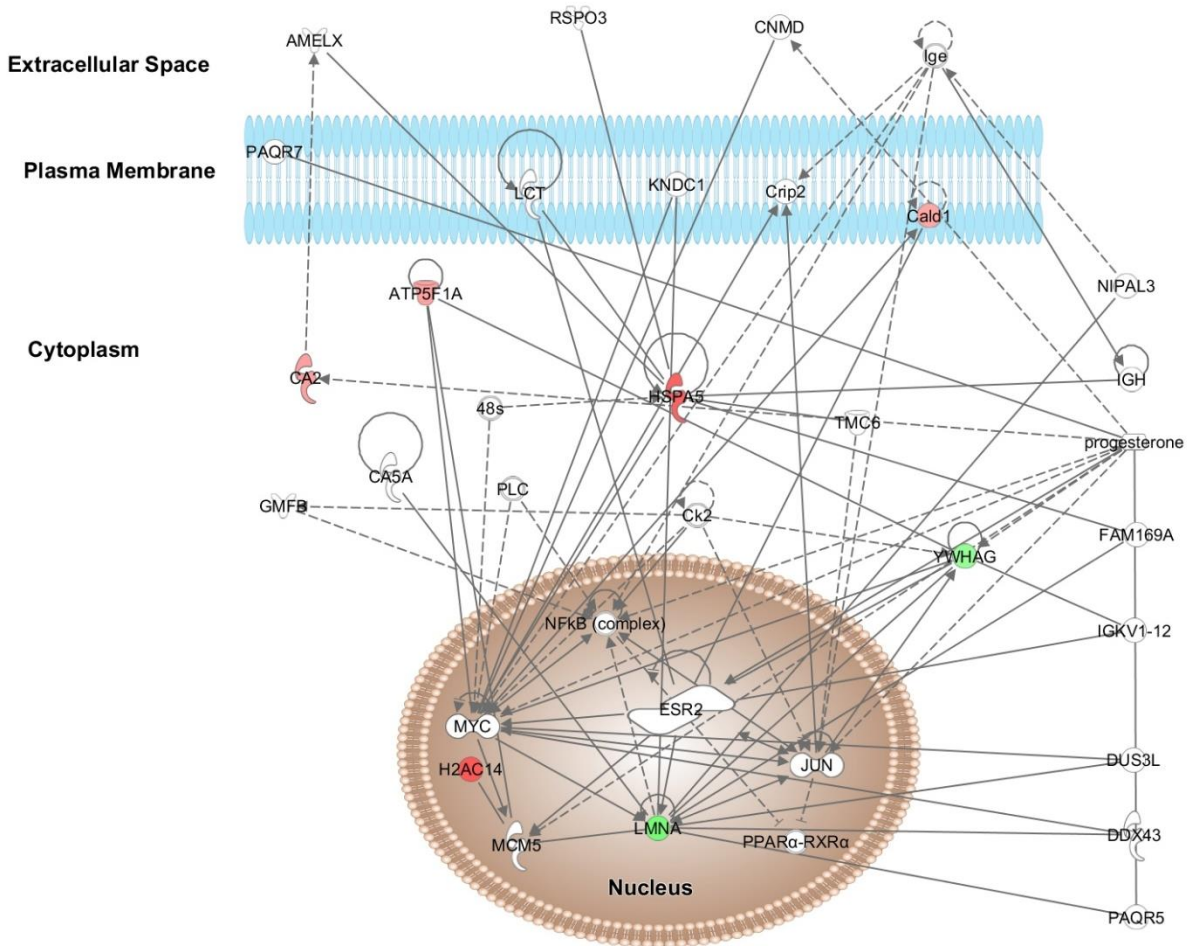

Figure 1. IPA® network linked to developmental disorder, hematological disease, and organismal injury and abnormalities. The network was assembled from E2-regulated proteins in the uterus of OVX mouse through identification by label-free shotgun proteomics. This network shows a relationship with estrogen receptor 2 (ESR2) in the nucleus, which can bind E2 to initiate gene transcription. Red symbols: upregulated, green symbols: downregulated by the hormone; solid lines: direct relationship, dashed line: indirect relationship.

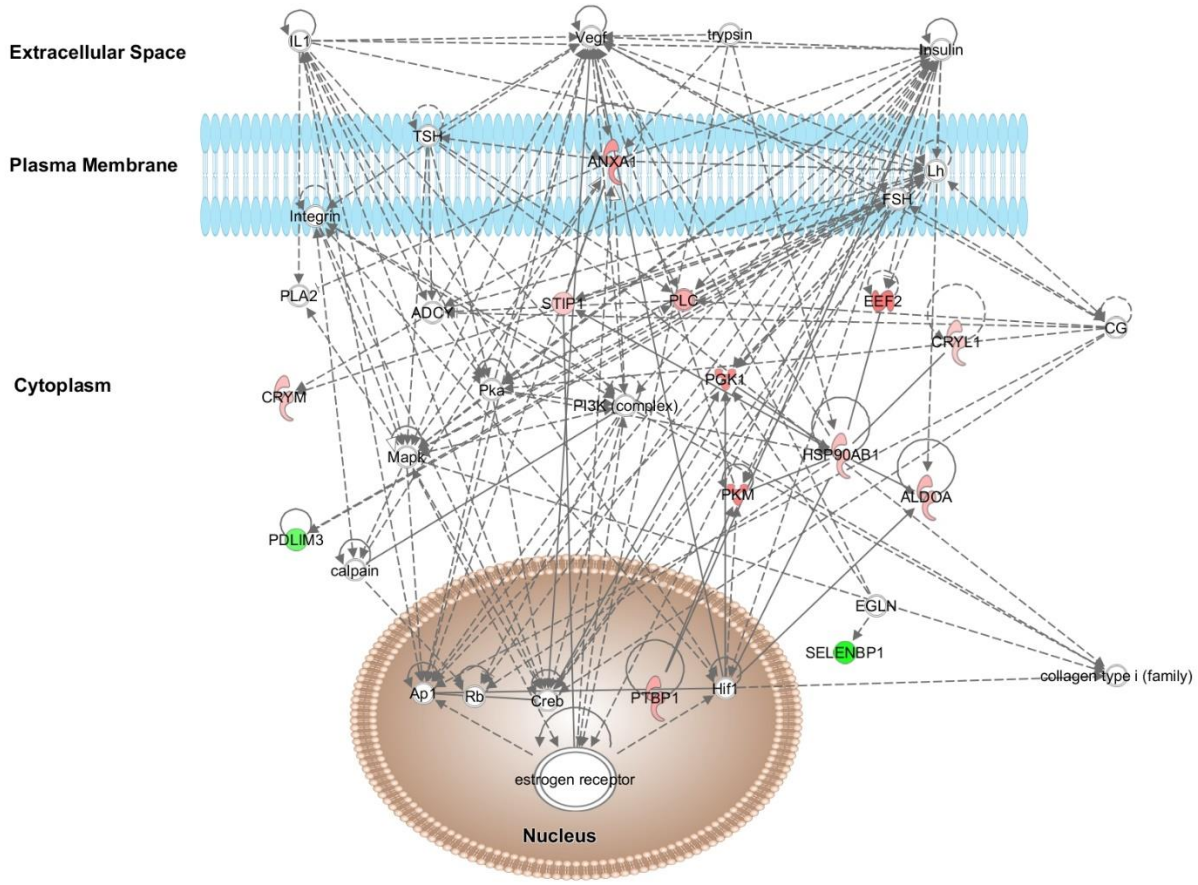

Figure 2. IPA® network linked to cancer, gastrointestinal disease, and hepatic system disease. The network was assembled from E2-regulated proteins in the uterus of OVX rats through identification by label-free shotgun proteomics. Red symbols: upregulated, green symbols: downregulated by the hormone; solid lines: direct relationship, dashed line: indirect relationship. Of note, this network shows the relationship between the proteins identified and links changes of protein expression links changes of levels in part to estrogen receptor signaling from the nuclei of the cells. These proteins could be potential targets of further targeted proteomic experiments.

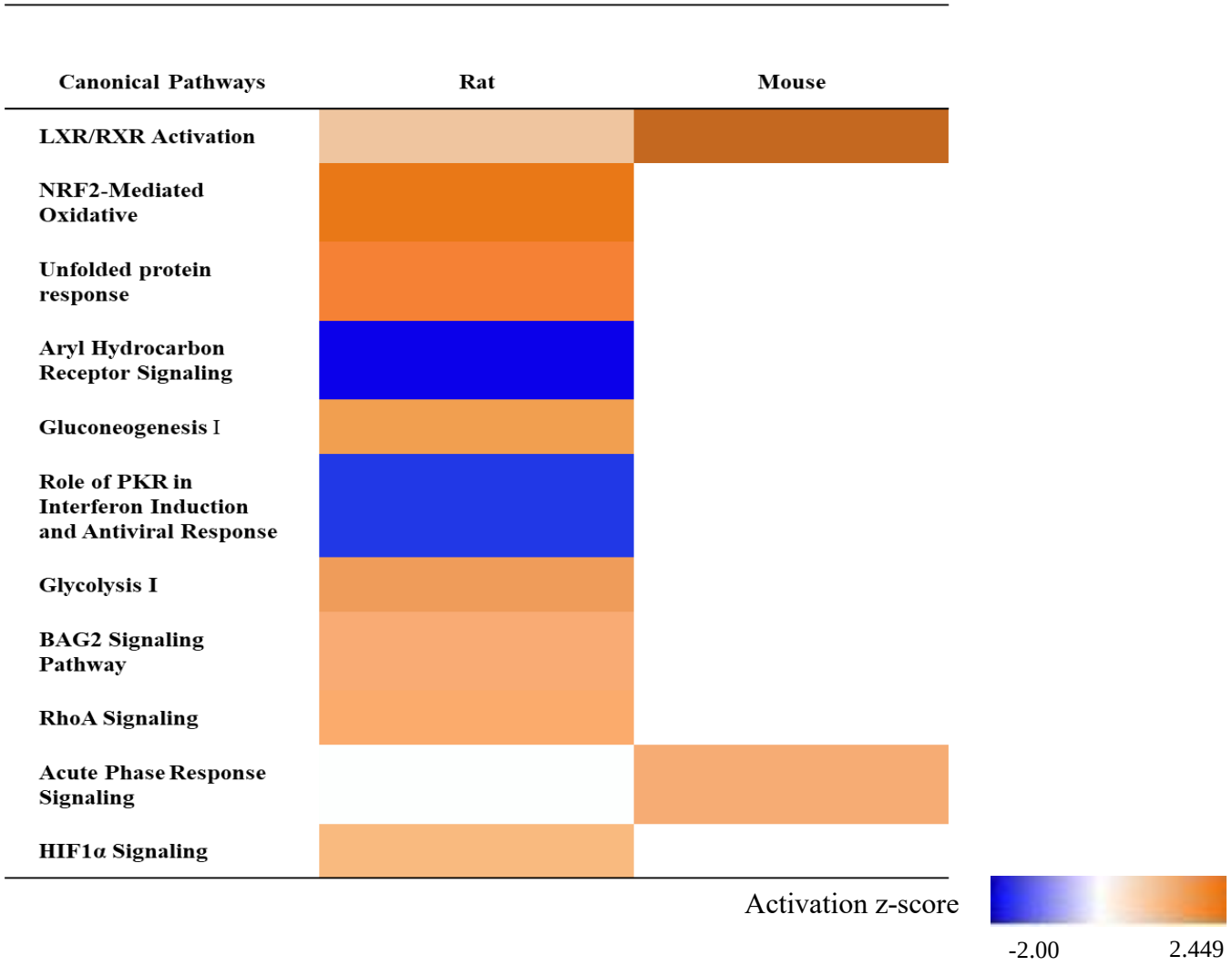

Figure 3. Comparative heatmap of canonical pathways between OVX mice and rats created by IPA®. Z-score infers the activation states of implicated biological functions. Orange: activation, blue: inhibition. Cutoff value was set to log p = 3.5.

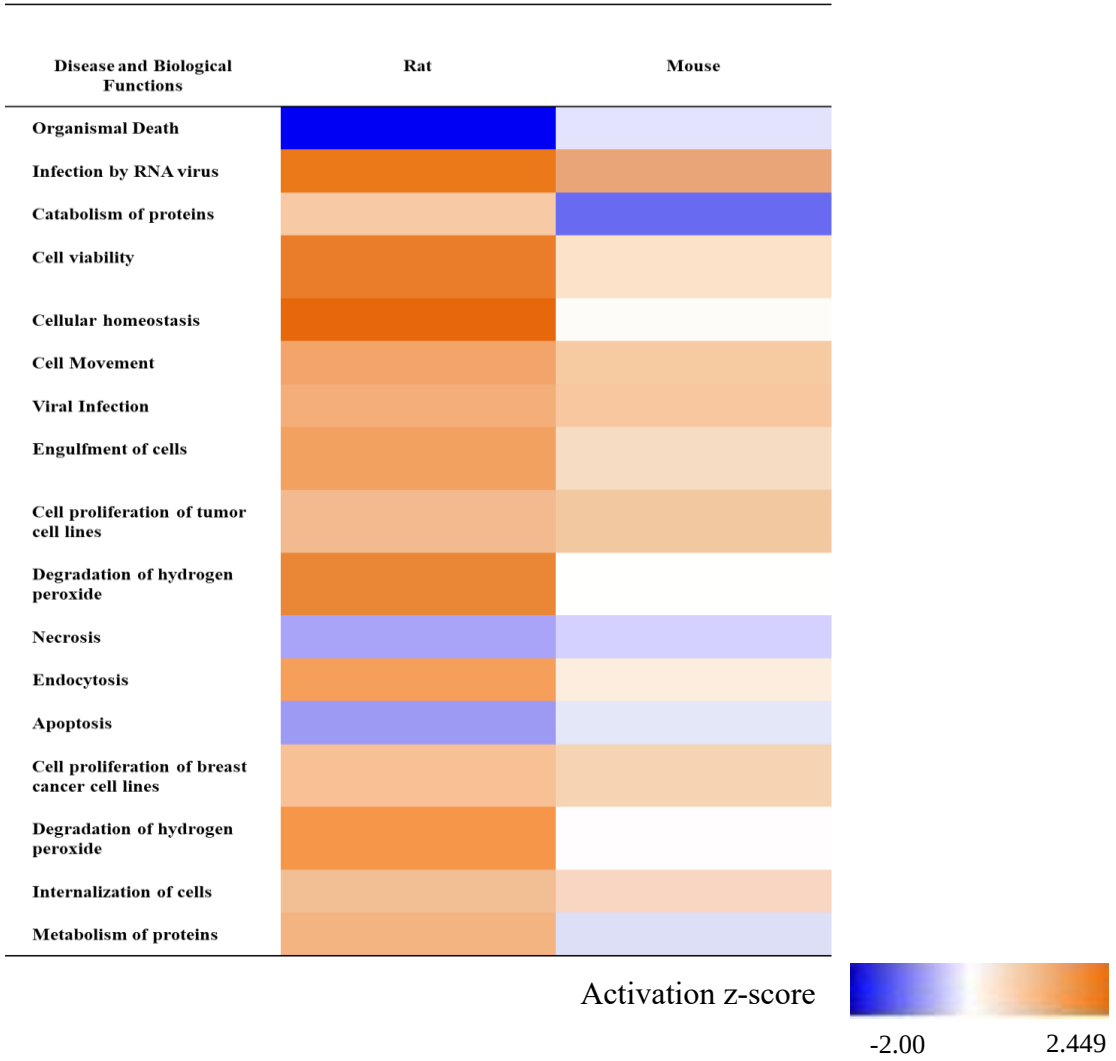

Figure 4. Comparative heatmap of disease and biological functions between OVX mice and rats created by IPA®. Z-score infers the activation states of implicated biological functions. Orange: activation, blue: inhibition. Cutoff value was set to log p = 6.

APPENDIX

Table S1. Proteins found upregulated by E2 in the OVX mouse uterus analyzed using MaxQuant and LFQ Analyst.

Gene Name	Protein IDs	Log fold change	p-value
Rplp1	P47955	1.09	9.63E-03
Nme2	Q01768	1.1	1.28E-02
Tubb5	P99024	1.17	2.81E-02
Gc	P21614	1.2	2.76E-02
Cald1	E9QA15	1.23	7.47E-03
Serpina1c	Q00896	1.39	2.57E-02
Ca2	P00920	1.59	2.80E-03
Kng1	O08677	1.59	1.74E-03
Tubb4b	P68372	1.67	5.77E-04
Eef2	P58252	1.71	4.18E-03
Tgm2	P21981	1.72	2.78E-03
Atp5a1	Q03265	1.8	2.69E-03
Apoa2	P09813	1.87	1.15E-02
Des	P31001	1.92	5.58E-05
Pkm	P52480	1.92	1.93E-05
Pdia6	Q922R8	1.99	3.26E-04
Hsp90b1	P08113	2.12	2.90E-04

Serpina3k	P07759	2.15	6.85E-03
Gnb2l1	P68040	2.26	1.90E-03
Hpx	Q91X72	2.38	5.20E-03
Serpinh1	P19324	2.41	1.15E-03
Hspa5	P20029	2.45	6.91E-05
C3	P01027	2.9	1.40E-05
Hist1h2af	Q8CGP5	2.93	9.04E-06
Apoa1	Q00623	3.2	1.29E-03
Flna	Q8BTM8	3.31	6.86E-07
Eef1a1	P10126	3.45	1.87E-06
Myh11	A0A2R8VHF9	3.49	1.10E-09

Table S2. Proteins found downregulated by E2 in the OVX mouse uterus analyzed using MaxQuant and LFQ Analyst.

Gene Name	Protein IDs	Log fold change	p-value
Lmnb1	P14733	-3.41	8.14E-08
Ptrf	O54724	-3.23	8.89E-09
Gstm1	P10649	-2.91	2.79E-09
Tpi1	P17751	-2.79	3.42E-03
Sod1	P08228	-2.68	3.39E-06
Pebp1	P70296	-2.61	1.92E-04
Mdh1	P14152	-2.6	3.46E-08
Prelp	Q9JK53	-2.56	1.38E-07
Anxa6	P14824	-2.38	4.82E-07
Gstp1	P19157	-2.34	7.78E-05
Pdlim3	O70209	-2.18	3.92E-03
Lmna	P48678	-2.11	1.83E-08
Ywhag	P61982	-2.1	7.26E-04

Ahnak2	F7CVJ5	-2.09	1.95E-07
Vcl	Q64727	-2.09	2.64E-05
Prdx6	O08709	-2.01	2.91E-03
Ogn	Q62000	-1.76	7.23E-03
Anxa2	P07356	-1.61	1.80E-02
Hbb-b2	P02089	-1.58	2.94E-03
Mif	P34884	-1.55	3.41E-03
Glo1	Q9CPU0	-1.53	1.92E-02
Lum	P51885	-1.47	1.21E-03
Tagln2	Q9WVA4	-1.45	5.23E-03
Dcn	P28654	-1.28	5.12E-03
Pgk1	P09411	-1.22	2.77E-02
Ca3	P16015	-1.17	1.88E-02
P0DP28	P0DP28	-1.12	4.79E-05
Lgals1	P16045	-1.11	1.18E-03
Park7	Q99LX0	-1.06	2.66E-03

Table S3. Proteins found upregulated by E2 in the OVX rat uterus analyzed using MaxQuant and LFQ Analyst.

Gene Name	Protein ID	Log Fold Change	p-Value
Clic1	Q6MG61	1.01	0.00493
Tpm3	Q63610	1.01	0.0122
G6pdx	P05370	1.07	0.0015
Gpx1	P04041	1.08	0.000975
Atic	O35567	1.09	0.00565
Vcl	P85972	1.09	0.0218
Anxa5	P14668	1.1	0.00764
Msn	O35763	1.1	0.00455
Pgm1	Q499Q4	1.1	0.00227
Cct2	Q5XIM9	1.14	0.00226
Cox6b1	D3ZD09	1.19	0.0035
Tubb5	P69897	1.19	0.00292
Alb	P02770	1.22	0.00149
Eif4a1	Q6P3V8	1.25	0.0124
Psap	P10960	1.29	0.00115
Ctsh	P00786	1.33	0.0182

Calr	P18418	1.38	0.0125
Pgls	P85971	1.39	0.00556
Pycard	G3V8L1	1.39	4.62E-05
Rps7	P62083	1.39	0.000714
Tln1	G3V852	1.43	0.000365
Itih4	Q5EBC0	1.44	0.000984
Akr1a1	P51635	1.45	0.00103
Prdx1	Q63716	1.51	0.00989
Tagln	P31232	1.51	0.000353
Cryl1	Q811X6	1.52	0.0222
Mdh2	P04636	1.52	0.00349
Stip1	O35814	1.55	0.000324
Rpl12	P23358	1.57	4.24E-06
Psme1	Q6P9V7	1.58	0.00114
Ube2n	Q9EQX9	1.58	0.00357
Ppp1cb	P62142	1.59	0.000146
Prdx3	Q9Z0V6	1.6	0.0083
A1m	Q63041	1.61	0.00239
Hspa4	O88600	1.61	0.000452

Cfl1	P45592	1.63	0.00347
Cycs	P62898	1.63	0.000283
Hsp90aa1	P82995	1.64	0.00184
Hspd1	P63039	1.64	8.75E-05
alf-c1	O88311	1.65	7.08E-07
Gapdh	P04797	1.68	8.12E-07
Hspa5	P06761	1.69	0.00166
Gc	Q68FY4	1.71	0.00297
Tkt	P50137	1.71	0.000784
Lcp1	Q5XI38	1.75	0.00835
Sod1	P07632	1.76	0.000609
Dbi	P11030	1.78	0.000917
Dstn	Q7M0E3	1.78	0.00734
Pdia6	Q63081	1.79	0.00302
Crym	Q9QYU4	1.81	9.60E-06
Gpi	Q6P6V0	1.82	0.00446
Hsp90ab1	P34058	1.84	0.0021
Ywhah	P68511	1.88	2.17E-05
Ran	P62828	1.91	1.53E-06

Cndp2	Q6Q0N1	1.97	4.09E-07
Ass1	P09034	1.98	1.46E-06
Ppib	P24368	1.98	3.77E-06
Prelp	Q9EQP5	2	0.000779
Capg	Q6AYC4	2.06	7.47E-06
Des	Q6P725	2.07	2.49E-05
Aldoa	P05065	2.09	0.00254
Ctsb	Q6IN22	2.1	0.0149
Lpo	D4A400	2.13	7.13E-05
Naca	M0R9L0	2.13	4.07E-05
Txnrd1	O89049	2.18	1.41E-06
Nme2	P19804	2.27	3.25E-06
Pdia3	P11598	2.28	0.00733
Actr3	Q4V7C7	2.33	6.10E-08
Pgd	P85968	2.39	2.12E-08
Ezr	P31977	2.44	3.43E-09
Lmna	G3V8L3	2.45	5.49E-07
Tuba1b	Q6P9V9	2.45	2.53E-06
Ptbp1	Q00438	2.48	1.49E-07

C3	M0RBF1	2.55	0.000689
Arhgdib	Q5M860	2.57	0.00322
Lta4h	P30349	2.59	5.24E-07
Tf	P12346	2.61	0.00166
Sfn	G3V9A3	2.67	4.67E-06
Cap1	Q08163	2.68	2.99E-05
Actn4	Q9QXQ0	2.7	1.77E-07
Atp5a1	P15999	2.7	7.06E-07
Cs	G3V936	2.78	1.02E-05
Eef1b2	B5DEN5	2.85	2.60E-06
Hsp90b1	Q66HD0	2.85	7.16E-06
Anxa1	P07150	2.97	1.56E-10
Hist1h2bk	G3V9C7	3.13	0.000346
S100a6	P05964	3.24	2.29E-05
Vcp	P46462	3.26	7.79E-09
Krt7	G3V712	3.28	5.68E-09
Pgk1	P16617	3.36	3.98E-06
Serpinh1	Q5RJR9	3.45	2.97E-09
Krt8	Q10758	3.51	2.68E-08

Pkm	P11980-2	3.61	4.42E-06
Eef2	P05197	3.87	4.56E-09
Krt19	Q63279	4.67	2.23E-11
Tgm2	Q9WVJ6	4.79	1.91E-11
Eef1a1	P62630	5.25	5.05E-07
S100g	P02634	5.82	1.49E-13
Ldha	P04642	5.87	6.97E-09

Table S4. Proteins found downregulated by E2 in the OVX rat uterus analyzed using MaxQuant and LFQ Analyst.

Gene Name	Protein IDs	log fold change	p-value
Selenbp1	Q8VIF7	-3.63	7.23E-09
Crp	P48199	-3.58	4.81E-09
Banf1	Q9R1T1	-3.52	0.000325
Hdgf	Q8VHK7	-3.49	3.68E-05
Rbp1	P02696	-2.82	1.50E-05
Dpp7	Q9EPB1	-2.65	4.39E-08
n/a	A0A0G2JTW9	-2.62	0.00248
Ca2	P27139	-2.6	0.000923
Mcam	Q9EPF2-2	-2.54	0.000489
Pdlim3	A0A0G2JSM3	-2.45	0.00198
Lum	P51886	-2.07	8.82E-08
Ddah2	Q6MG60	-2.04	0.00894
Eno2	P07323	-1.96	0.00072
Glo1	Q6P7Q4	-1.93	0.000553

Pebp1	P31044	-1.93	6.39E-07
Fabp4	P70623	-1.82	0.0121
Nutf2	P61972	-1.75	0.0151
Ca1	B0BNN3	-1.74	0.0085
Ahcy	P10760	-1.72	0.00444
Glod4	Q5I0D1	-1.66	0.000269
Mif	P30904	-1.57	9.71E-05
Sh3bgrl	B5DFD8	-1.57	6.57E-07
Lmnb1	P70615	-1.56	0.0106
Gda	Q9WTT6	-1.48	0.011
Hbb	P02091	-1.4	0.00169
Serpina1	P17475	-1.35	0.00509
Mylk	D3ZFU9	-1.17	0.00461
Ptms	P04550	-1.1	0.00912

Figure S1. LFQ Analyst analysis of OVX mice results. There were 59 significant differentially expressed proteins, 30 downregulated, and 29 upregulated. (**a**) Volcano plot of the proteins found to be significantly regulated. (**b**) Protein plot of two proteins of interest: lumican and transglutaminase 2.

(**a**)

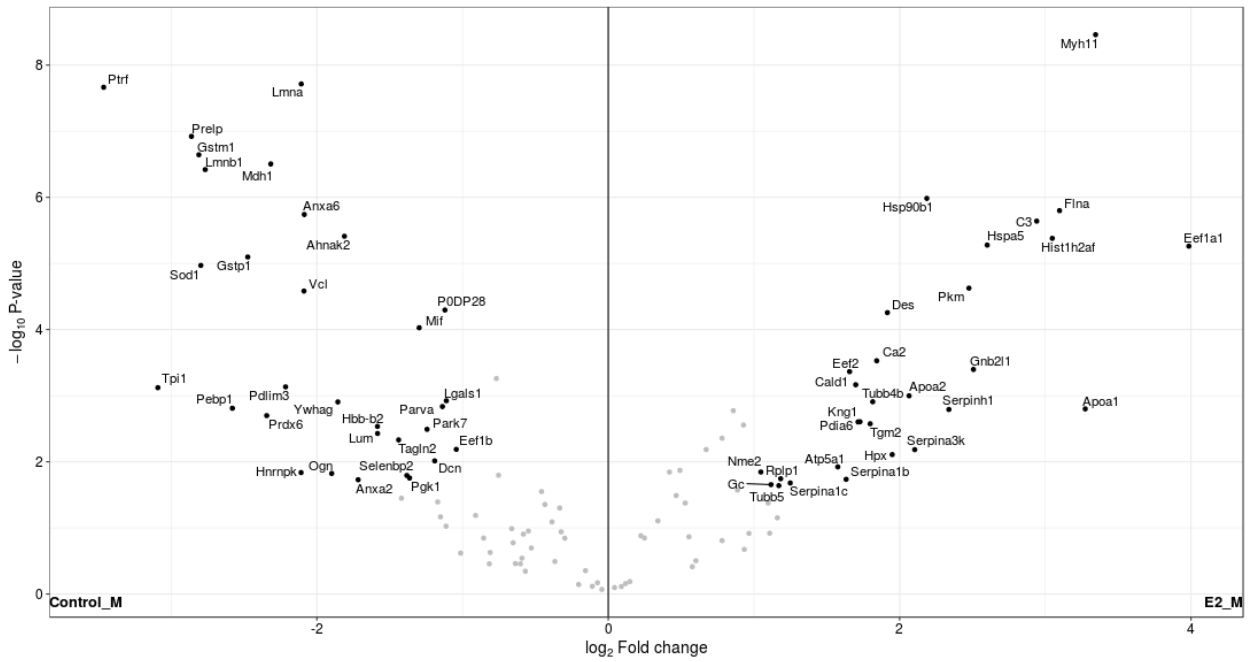

(**b**)

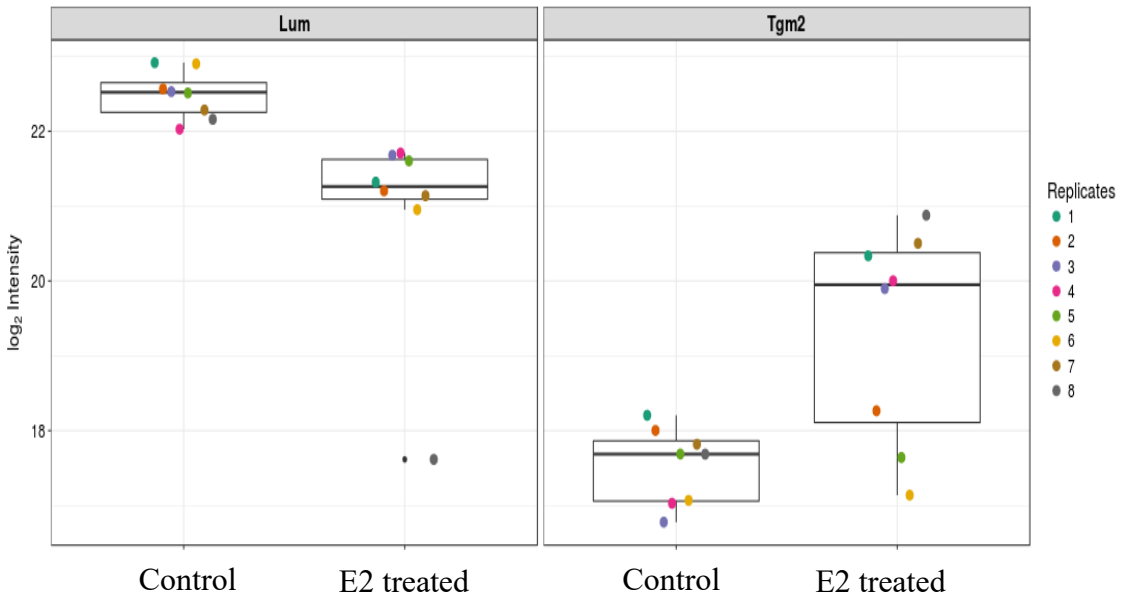

Figure S2. LFQ Analyst analysis of OVX rats results. There were 126 significant differentially expressed proteins, 28 downregulated, and 98 upregulated. (**a**) Volcano plot of the proteins found to be significantly regulated. (**b**) Protein plot of two proteins of interest: lumican and transglutaminase 2.

(**a**)

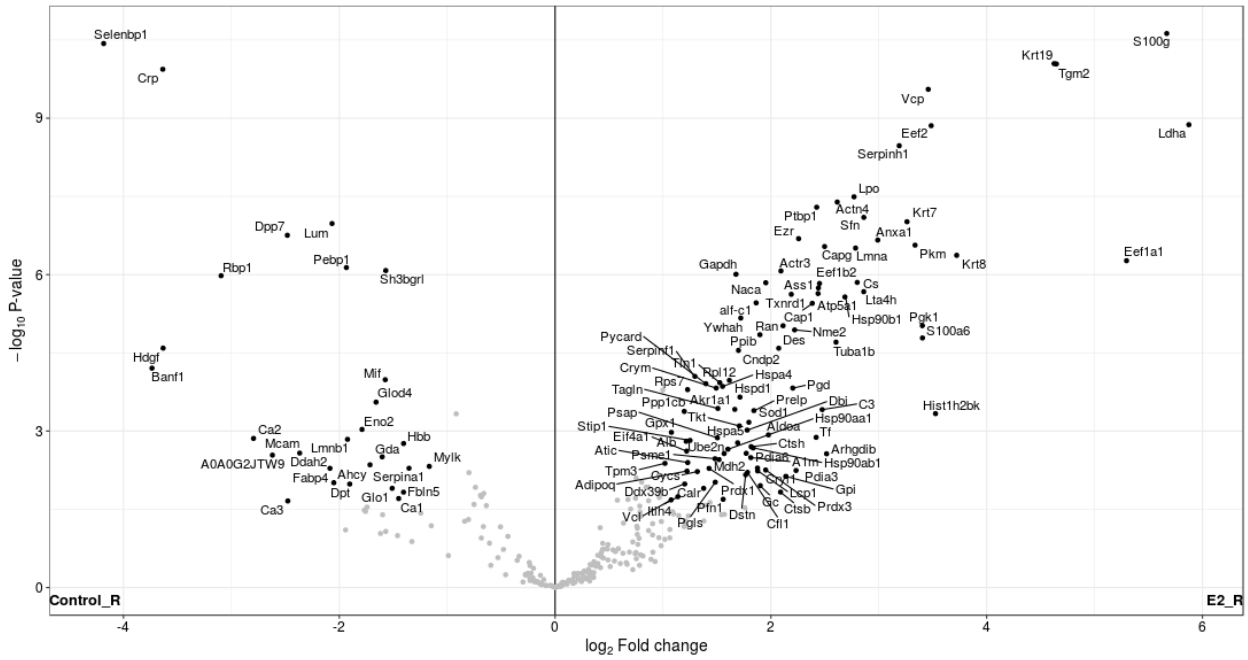

(**b**)

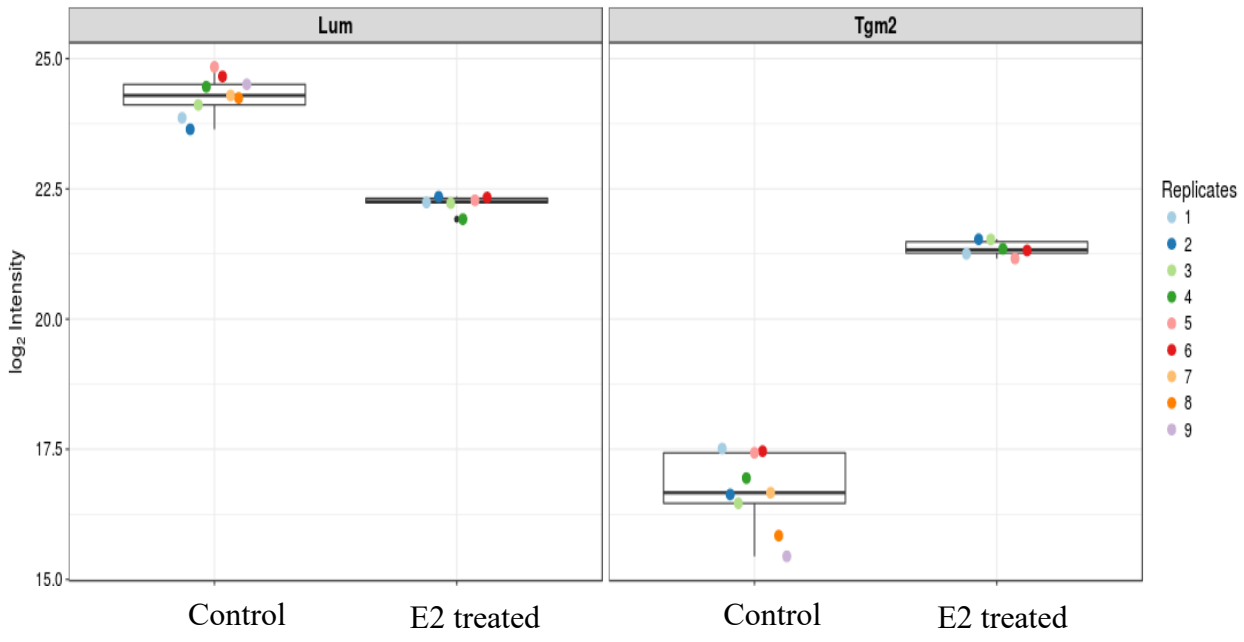

Table S5. Comparison of the networks generated using IPA®. Bolded numbered networks show interactions with estrogen receptor 2 located in the nucleus.

Mouse IPA Networks		**Rat IPA Networks**	
1	Metabolic Disease, Neurological Disease, Protein Synthesis	1	Cell Morphology, Cellular Assembly and Organization, Cellular Function and Maintenance
2	Cancer, Gastrointestinal Disease, Infectious Diseases	2	Drug Metabolism, Free Radical Scavenging, Small Molecule Biochemistry
3	Drug Metabolism, Endocrine System Disorders, Glutathione Depletion in Liver	3	Cancer, Gastrointestinal Disease, Hepatic System Disease
4	Development Disorder, Hematological Disease, Organismal Injury and Abnormalities	4	Humoral Immune Response, Neurological Disease, Organismal Injury and Abnormalities
		5	Cancer, Gastrointestinal Disease, Hepatic System Disease
		6	Cell-To-Cell Signaling and Interaction, Molecular Transport, Small Molecule Biochemistry
		7	Developmental Disorder, Ophthalmic Disease, Organismal Injury and Abnormalities

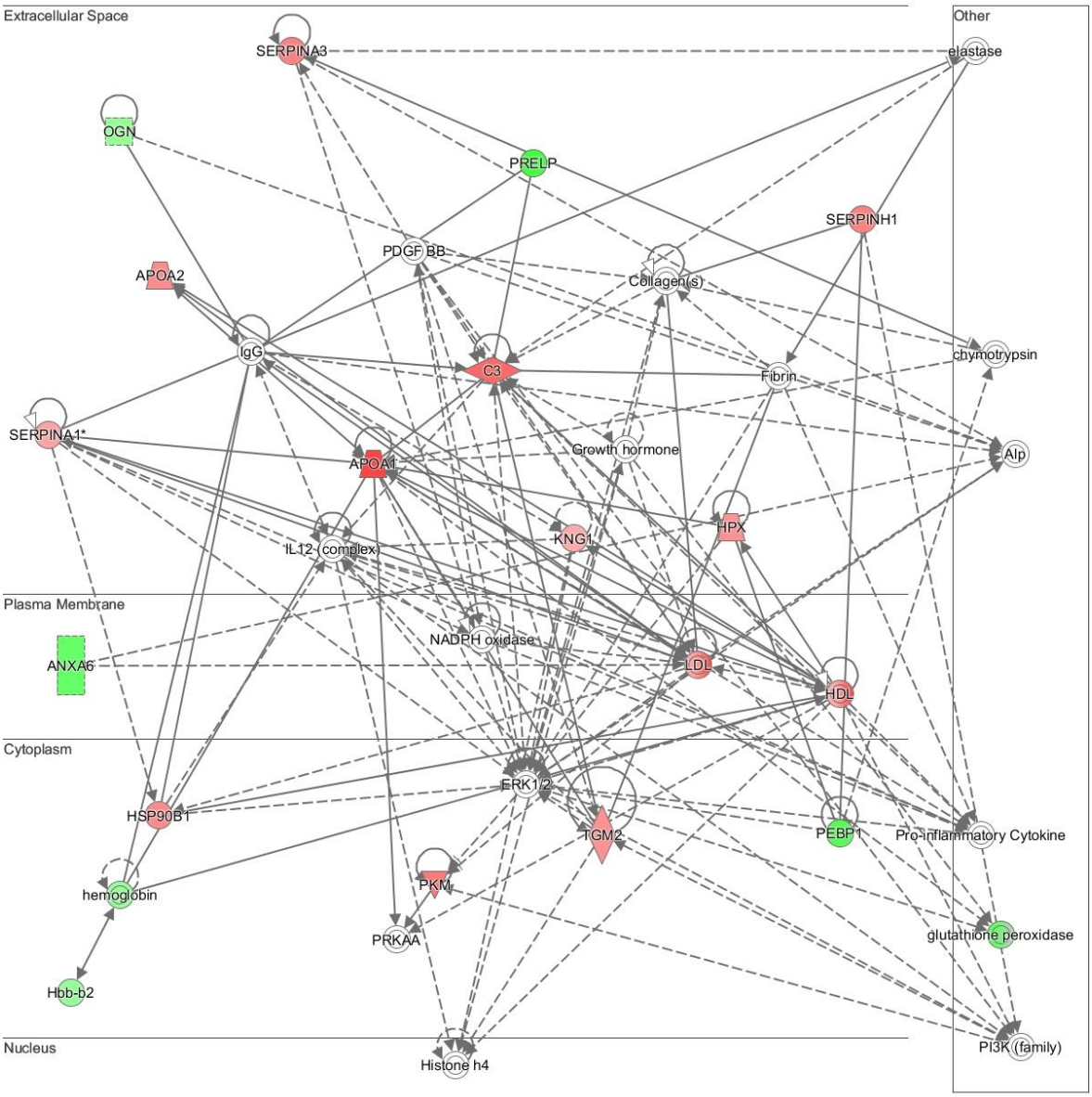

Figure S3. IPA® network linked to metabolic disease and protein synthesis. The network was assembled from E2-regulated proteins in the uterus of OVX mouse through identification by label-free shotgun proteomics. Red symbols: upregulated, green symbols: downregulated by the hormone; solid lines: direct relationship, dashed line: indirect relationship.

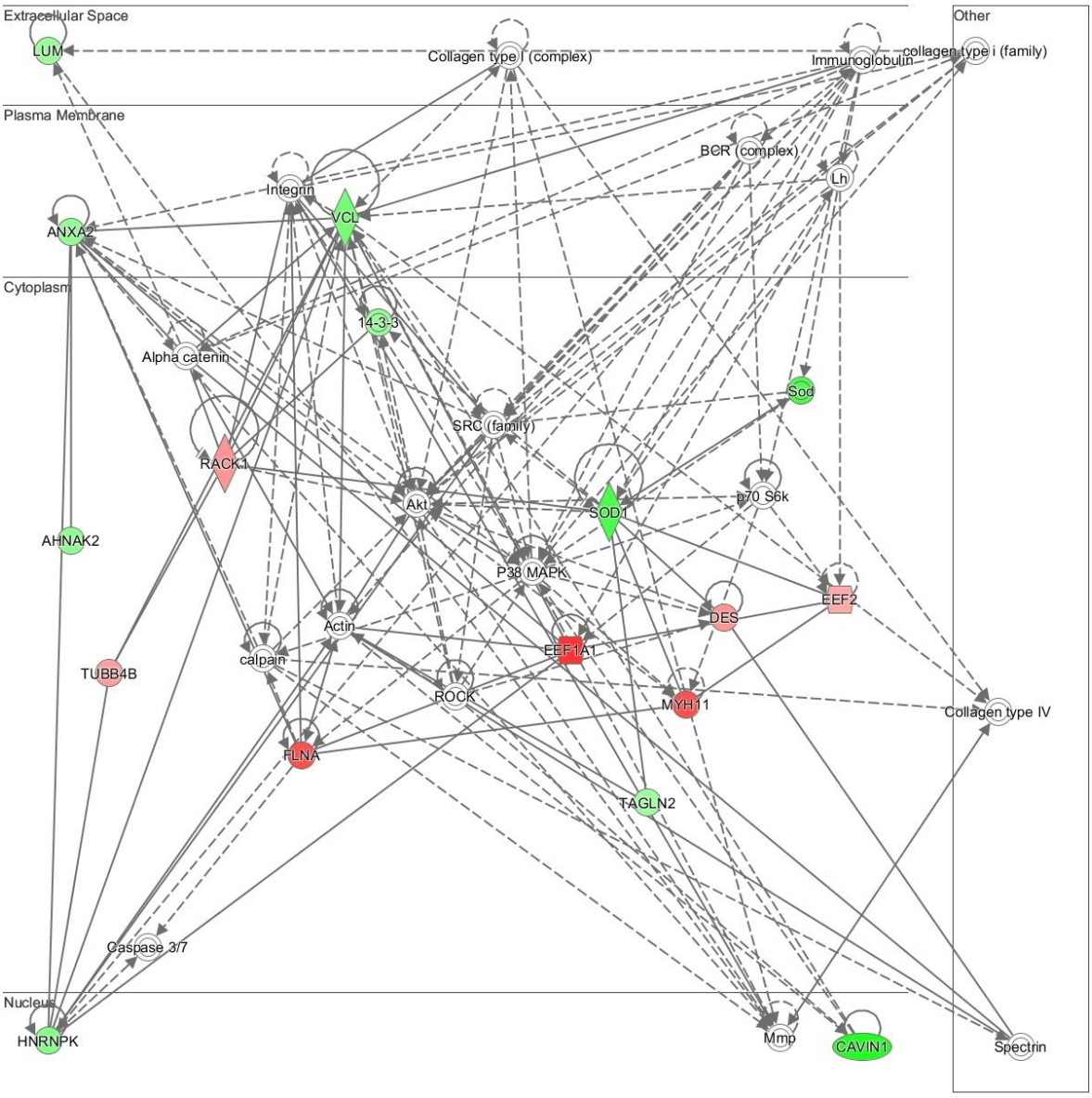

Figure S4. IPA® network linked to cancer, gastrointestinal disease, and infectious disease. The network was assembled from E2-regulated proteins in the uterus of OVX mouse through identification by label-free shotgun proteomics. Red symbols: upregulated, green symbols: downregulated by the hormone; solid lines: direct relationship, dashed line: indirect relationship.

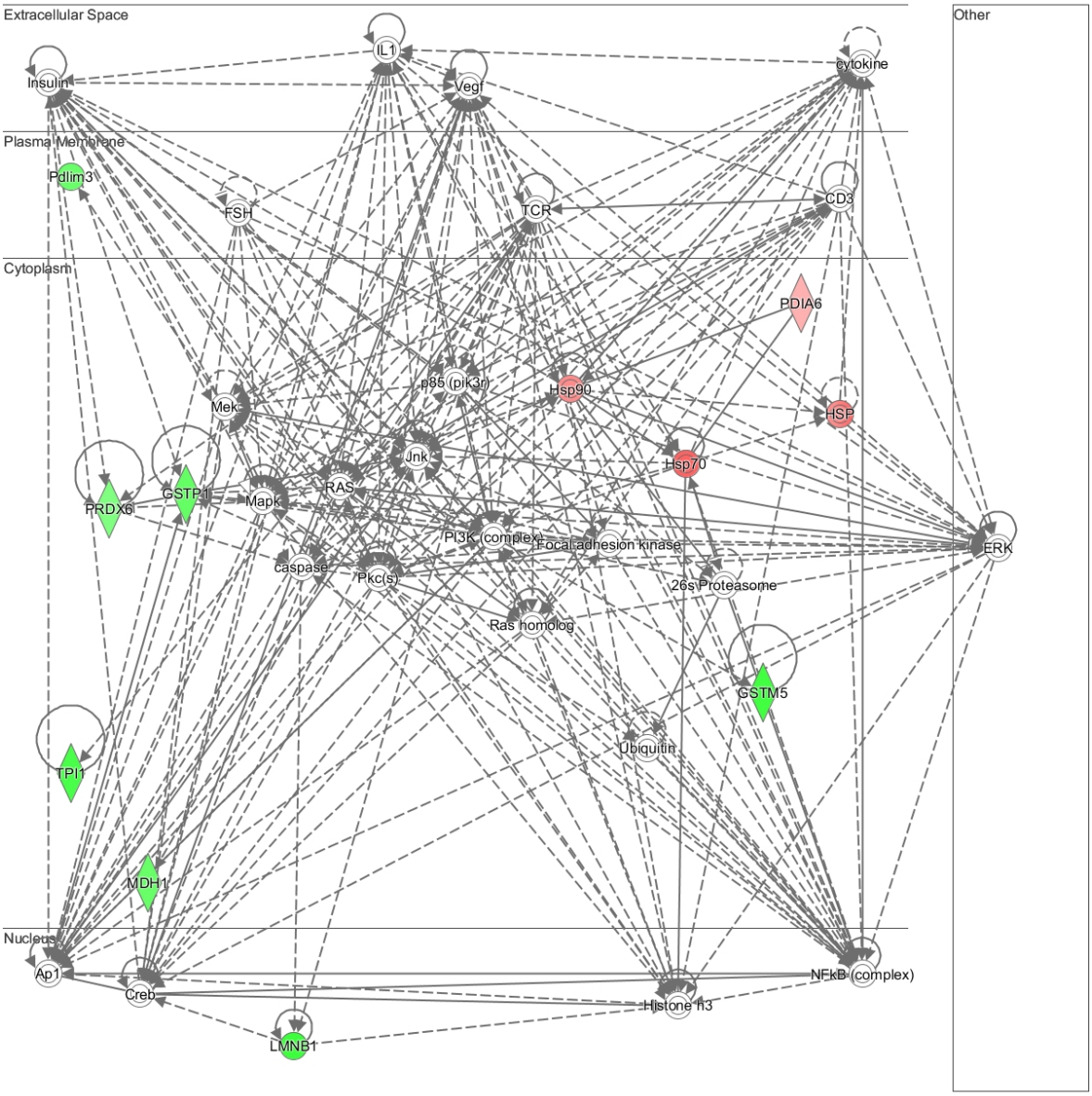

Figure S5. IPA® network linked to drug metabolism, endocrine system disorders, glutathione depletion. The network was assembled from E2-regulated proteins in the uterus of OVX mouse through identification by label-free shotgun proteomics. Red symbols: upregulated, green symbols: downregulated by the hormone; solid lines: direct relationship, dashed line: indirect relationship.

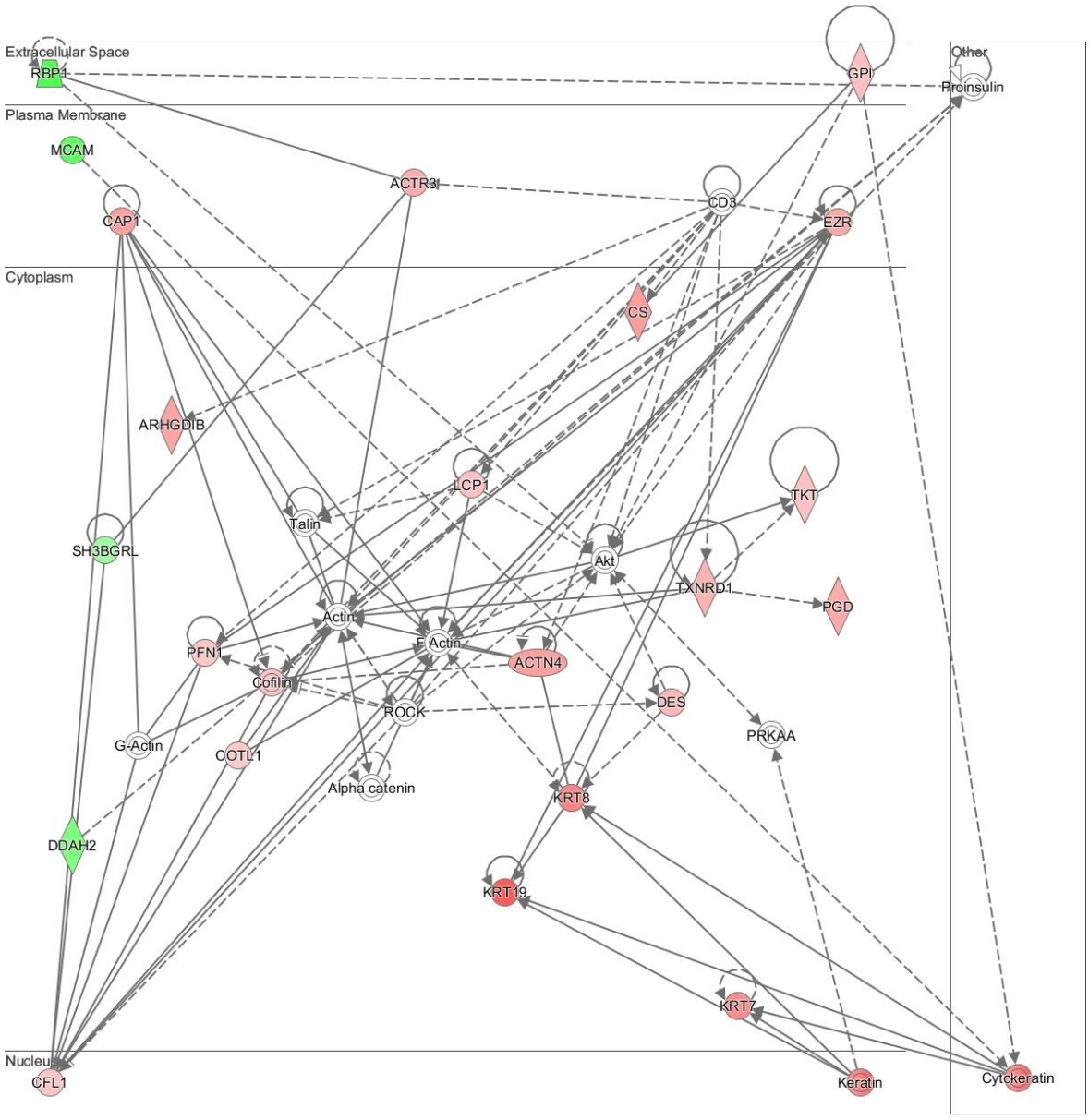

Figure S6. IPA® network linked to cell morphology, cell assembly and organization, cellular function and maintenance. The network was assembled from E2-regulated proteins in the uterus of OVX rats through identification by label-free shotgun proteomics. Red symbols: upregulated, green symbols: downregulated by the hormone; solid lines: direct relationship, dashed line: indirect relationship.

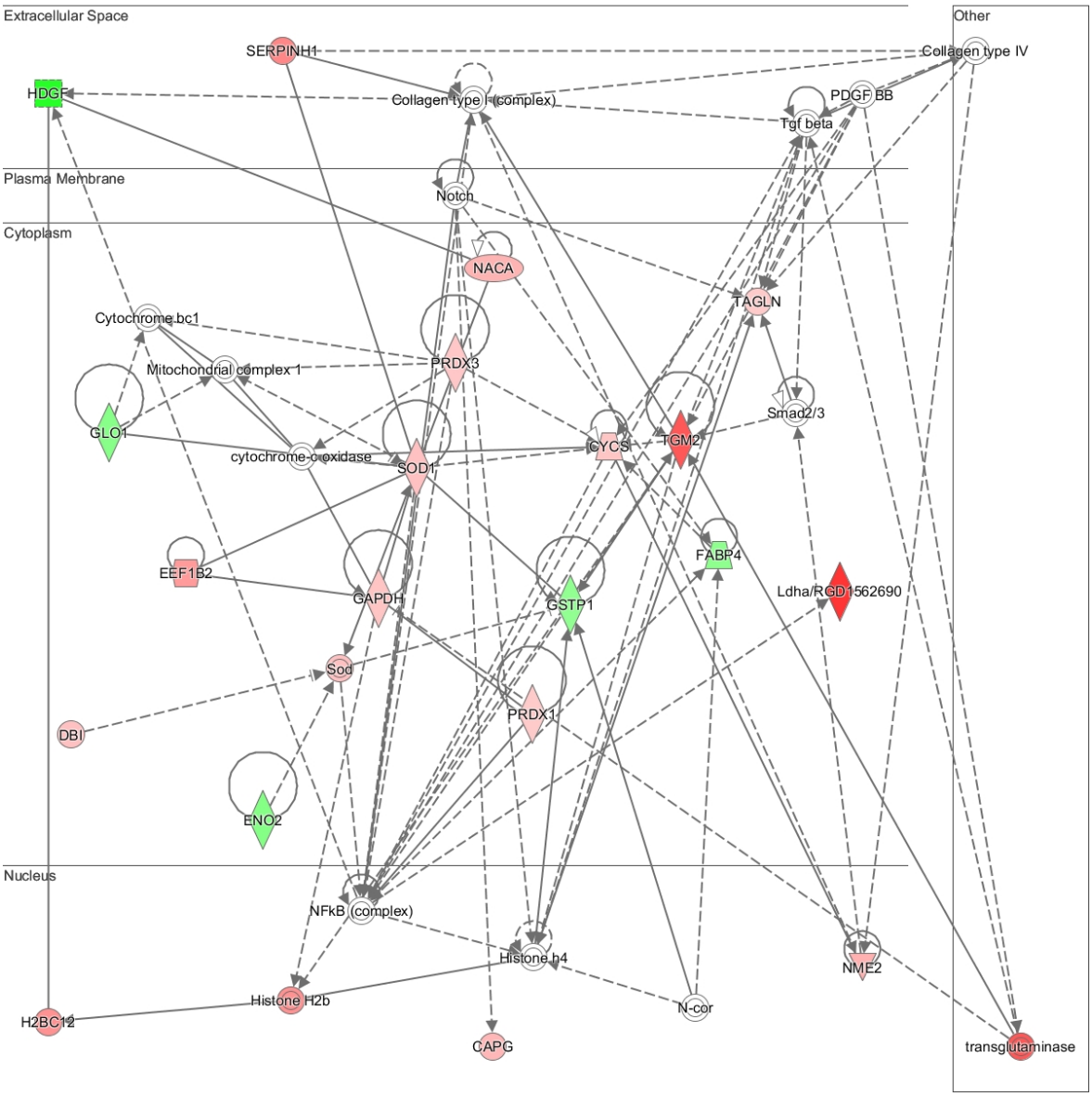

Figure S7. IPA® network linked to drug metabolism, free radical scavenging, small molecule biochemistry. The network was assembled from E2-regulated proteins in the uterus of OVX rats through identification by label-free shotgun proteomics. Red symbols: upregulated, green symbols: downregulated by the hormone; solid lines: direct relationship, dashed line: indirect relationship.

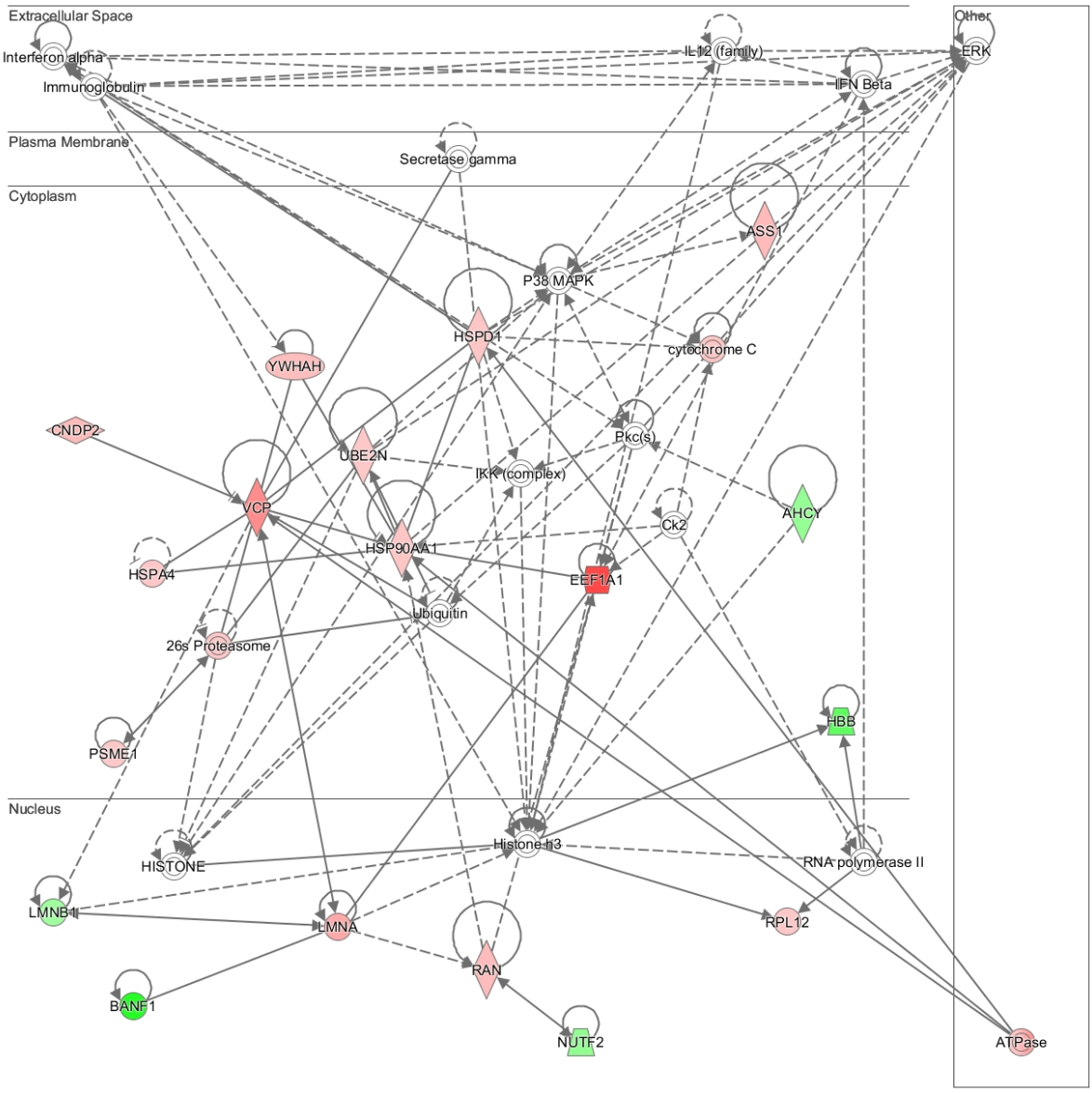

Figure S8. IPA® network linked to cancer, gastrointestinal disease, and hepatic system disease. The network was assembled from E2-regulated proteins in the uterus of OVX rats through identification by label-free shotgun proteomics. Red symbols: upregulated, green symbols: downregulated by the hormone; solid lines: direct relationship, dashed line: indirect relationship.

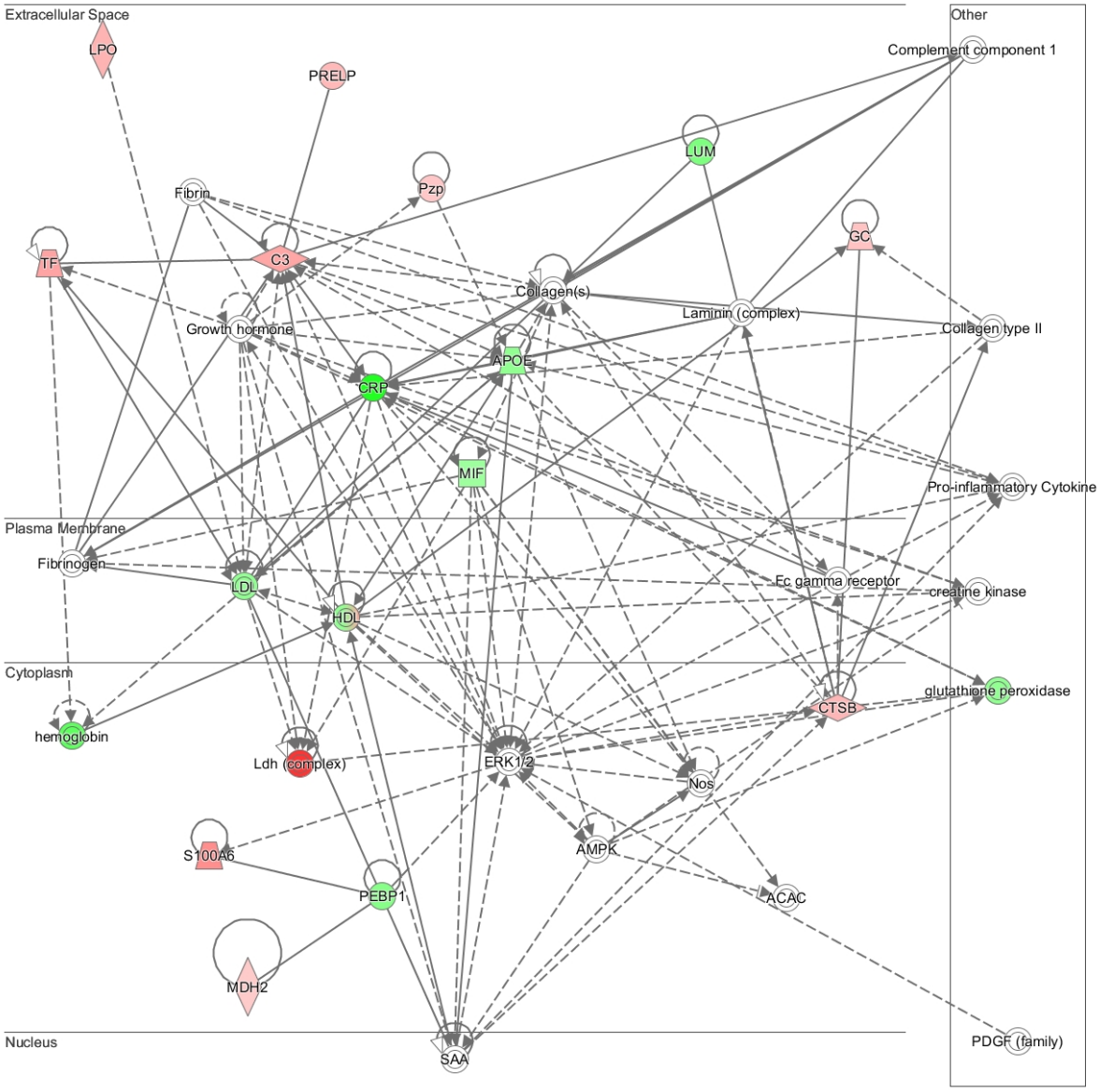

Figure S9. IPA® network linked to humoral immune response, organismal injury and abnormalities. The network was assembled from E2-regulated proteins in the uterus of OVX rats through identification by label-free shotgun proteomics. Red symbols: upregulated, green symbols: downregulated by the hormone; solid lines: direct relationship, dashed line: indirect relationship.

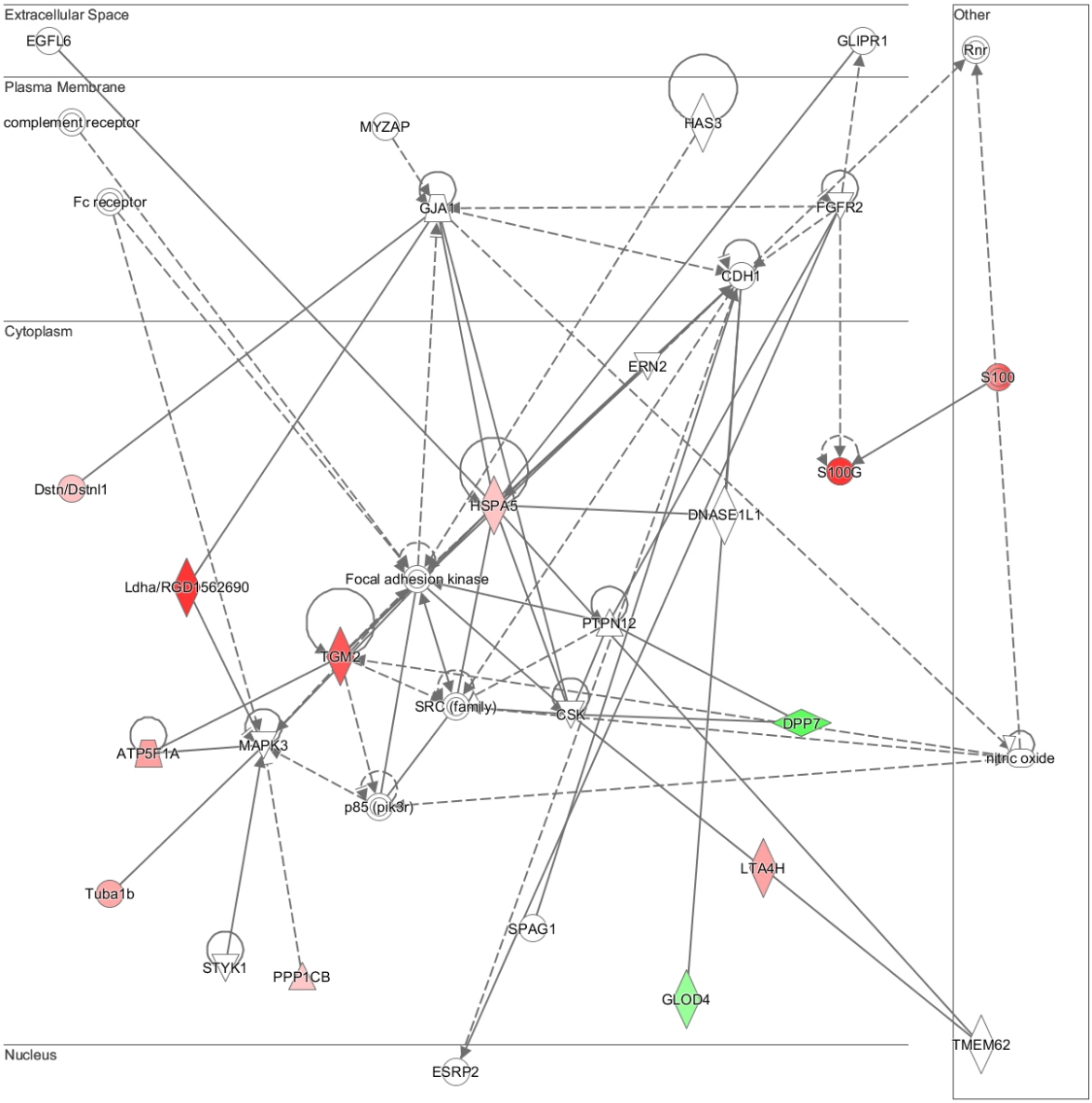

Figure S10. IPA® network linked to cell-to-cell signaling and interaction, molecular transport, and small molecule biochemistry. The network was assembled from E2-regulated proteins in the uterus of OVX rats through identification by label-free shotgun proteomics. Red symbols: upregulated, green symbols: downregulated by the hormone; solid lines: direct relationship, dashed line: indirect relationship.

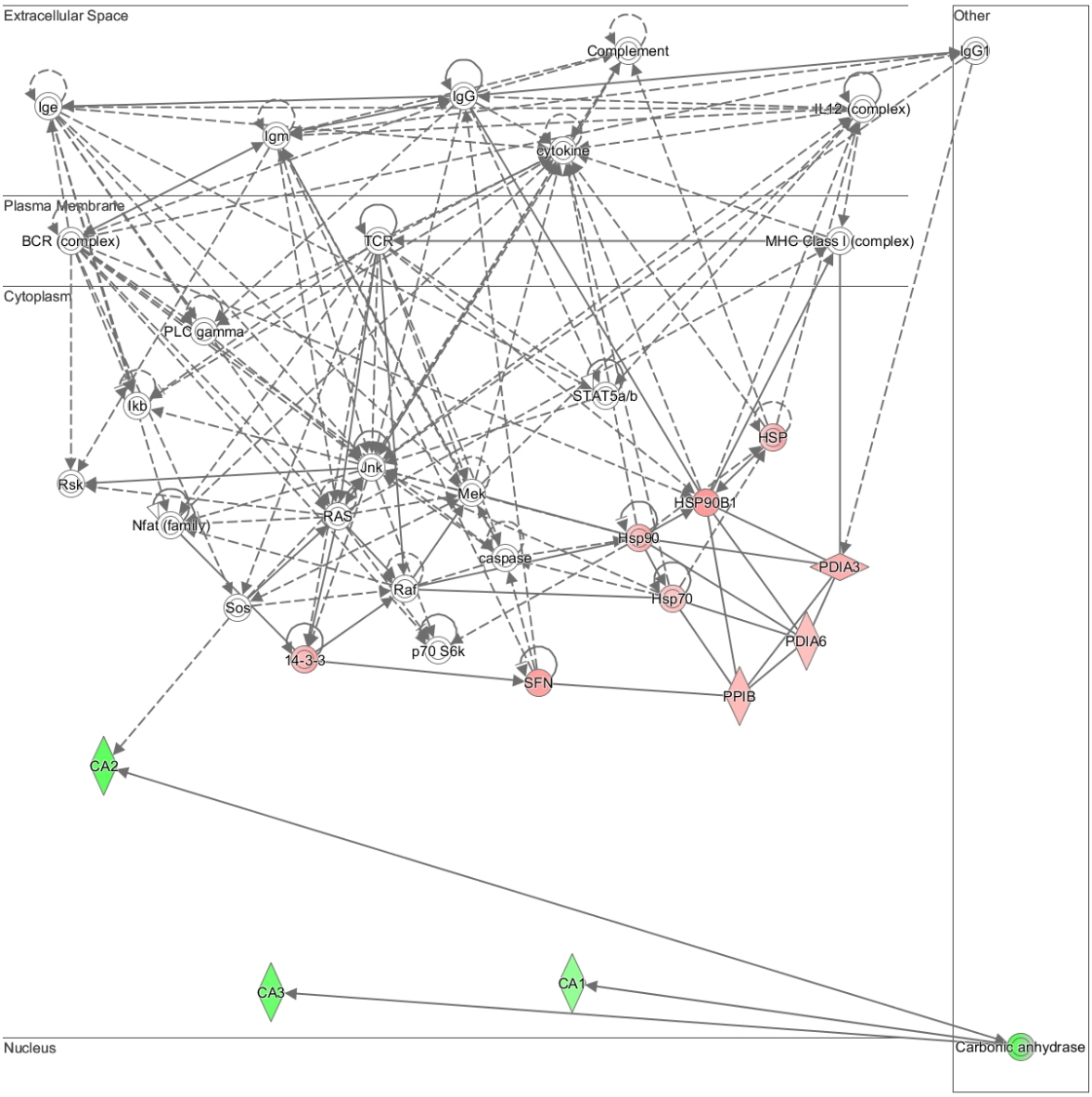

Figure S11. IPA® network linked to development disorder and organismal injury and abnormalities. The network was assembled from E2-regulated proteins in the uterus of OVX rats through identification by label-free shotgun proteomics. Red symbols: upregulated, green symbols: downregulated by the hormone; solid lines: direct relationship, dashed line: indirect relationship.

Table S6. Top canonical pathways found using IPA® assembled from E2-regulated proteins in the uterus of (**a**) OVX mice and (**b**) OVX rats through identification by label-free shotgun proteomics.

(**a**)

Canonical Pathways	p-value	Overlap
Acute Phase Response Signaling	4.03E-08	3.8% (7/182)
LXR/RXR Activation	1.26E-07	4.7% (6/128)
FXR/RXR Activation	1.89E-07	4.4% (6/137)
Unfolded protein response	1.51E-04	5.4% (3/56)
Aryl Hydrocarbon Receptor Signaling	1.62E-04	2.7% (4/149)

(**b**)

Canonical Pathways	p-value	Overlap
Glycolysis I	1.43E-09	23.1% (6/26)
Gluconeogenesis I	1.43E-09	21.1% (6/26)
Aldosterone Signaling in Epithelial Cells	5.40E-07	5.1% (8/158)
BAG2 Signaling Pathway	1.33E-06	11.6% (5/43)
HIF1 Signaling	3.81E-06	3.9% (8/205)

Table S7. Top molecular and cellular pathways found using IPA® assembled from E2-regulated proteins in the uterus of (**a**) OVX mice and (**b**) OVX rats through identification by label-free shotgun proteomics.

(**a**)

Molecular and cellular pathways	**p-value range**	**Number of molecules**
Cellular Compromise	5.18E-04 – 2.96E-14	22
Cellular Movement	4.18E-04 – 1.38E-11	28
Cell Death and Survival	5.90E-04 – 1.25E-10	31
Free Radical Scavenging	4.18E-04 – 3.21E-10	14
Cellular Function and Maintenance	5.55E-04 – 5.73E-10	33

(**b**)

Molecular and cellular functions	**p-value range**	**Number of molecules**
Cellular Movement	1.72E-05 – 6.01E-17	55
Cell Death and Survival	1.74E-05 – 2.30E-15	65
Cellular Compromise	1.54E-06 – 7.24E-13	31
Protein Synthesis	1.70E-06 – 1.01E-10	30
Free Radical Scavenging	1.88E-06 – 2.61E-10	24

Table S8. Top molecular and cellular functions found using IPA® assembled from E2-regulated proteins in the uterus of (**a**) OVX mice and (**b**) OVX rats through identification by label-free shotgun proteomics.

(**a**)

Physiological system development and function	**p-value range**	**Number of molecules**
Organismal Survival	8.31E-05 – 4.92E-08	25
Cardiovascular System Development and Function	5.36E-04 – 8.21E-08	23
Organismal Development	4.50E-04 – 8.47E-08	27
Tissue Development	5.00E-04 – 1.09E-07	24
Organ Development	4.02E-04 – 2.11E-07	18

(**b**)

Physiological system development and function	**p-value**	**Number of molecules**
Organismal Survival	1.24E-06 – 3.45E-11	46
Hematological System Development and Function	1.67E-05 – 1.79E-07	31
Immune Cell Trafficking	1.67E-05 – 1.79E-07	26
Tissue Development	1.70E-06 – 1.01E-10	30
Connective Tissue Development and Function	2.30E-06 – 1.62E-06	17

REFERENCES

1. Prokai L, Stevens SM, Jr., Rauniyar N, Nguyen V. Rapid label-free identification of estrogen-induced differential protein expression in vivo from mouse brain and uterine tissue. J Proteome Res. 2009;8(8):3862-71. Epub 2009/06/24. doi: 10.1021/pr900083v. PubMed PMID: 19545149; PubMed Central PMCID: PMCPMC2771330.
2. Rahlouni FR. Quantitative Proteomic Investigation of Estrogenic Endocrine Disrupting Effects in the Rat Uterus. University Of North Texas Graduate School of Biomedical Sciences 2016:1-159.
3. Kiernan UA. Biomarker rediscovery in diagnostics. Expert Opin Med Diagn. 2008;2(12):1391-400. Epub 2008/12/01. doi: 10.1517/17530050802566488. PubMed PMID: 23496785.
4. Graves PR, Haystead TA. Molecular biologist's guide to proteomics. Microbiol Mol Biol Rev. 2002;66(1):39-63; table of contents. Epub 2002/03/05. doi: 10.1128/mmbr.66.1.39-63.2002. PubMed PMID: 11875127; PubMed Central PMCID: PMCPMC120780.
5. Srinivas PR, Srivastava S, Hanash S, Wright GL, Jr. Proteomics in early detection of cancer. Clin Chem. 2001;47(10):1901-11. Epub 2001/09/25. PubMed PMID: 11568117.
6. Blackstock WP, Weir MP. Proteomics: quantitative and physical mapping of cellular proteins. Trends in Biotechnology. 1999;17(3):121-7. doi: 10.1016/s0167-7799(98)01245-1.
7. Basavaradhya Sahukar Shruthi PV, and Selvamani. Proteomics: A new perspective for cancer. Advanced Biomedical Research. 2016;5:67.
8. Callegari EA. Shotgun proteomics analysis of estrogen effects in the uterus using Two-Dimensional Liquid Chromatography and Tandem Mass Spectrometry. Springer New York; 2016. p. 131-48.
9. Wilm M. Quantitative proteomics in biological research. PROTEOMICS. 2009;9(20):4590-605. doi: 10.1002/pmic.200900299.
10. Patel VJ, Thalassinos K, Slade SE, Connolly JB, Crombie A, Murrell JC, et al. A comparison of labeling and label-free mass spectrometry-based proteomics approaches. J Proteome Res. 2009;8(7):3752-9. Epub 2009/05/14. doi: 10.1021/pr900080y. PubMed PMID: 19435289.
11. Rauniyar N. Parallel reaction monitoring: A targeted experiment performed using high resolution and high mass accuracy mass spectrometry. Int J Mol Sci. 2015;16(12):28566-81. Epub 2015/12/04. doi: 10.3390/ijms161226120. PubMed PMID: 26633379; PubMed Central PMCID: PMCPMC4691067.
12. Milac TI, Randolph TW, Wang P. Analyzing LC-MS/MS data by spectral count and ion abundance: two case studies. Stat Interface. 2012;5(1):75-87. Epub 2012/01/01. doi: 10.4310/SII.2012.v5.n1.a7. PubMed PMID: 24163717; PubMed Central PMCID: PMCPMC3806317.
13. Murray KK, Boyd RK, Eberlin MN, Langley GJ, Li L, Naito Y. Definitions of terms relating to mass spectrometry (IUPAC Recommendations 2013). Pure and Applied Chemistry. 2013;85(7):1515-609. doi: 10.1351/pac-rec-06-04-06.
14. Doerr A. Mass spectrometry–based targeted proteomics. Nature Methods. 2013;10(1):23-. doi: 10.1038/nmeth.2286.
15. Gallien S, Duriez E, Crone C, Kellmann M, Moehring T, Domon B. Targeted proteomic quantification on quadrupole-orbitrap mass spectrometer. Mol Cell Proteomics.

2012;11(12):1709-23. Epub 2012/09/11. doi: 10.1074/mcp.O112.019802. PubMed PMID: 22962056; PubMed Central PMCID: PMCPMC3518128.
16. Peterson AC, Russell JD, Bailey DJ, Westphall MS, Coon JJ. Parallel reaction monitoring for high resolution and high mass accuracy quantitative, targeted proteomics. Mol Cell Proteomics. 2012;11(11):1475-88. Epub 2012/08/07. doi: 10.1074/mcp.O112.020131. PubMed PMID: 22865924; PubMed Central PMCID: PMCPMC3494192.
17. Gallien S, Bourmaud A, Kim SY, Domon B. Technical considerations for large-scale parallel reaction monitoring analysis. J Proteomics. 2014;100:147-59. Epub 2013/11/10. doi: 10.1016/j.jprot.2013.10.029. PubMed PMID: 24200835.
18. Ronsein GE, Pamir N, von Haller PD, Kim DS, Oda MN, Jarvik GP, et al. Parallel reaction monitoring (PRM) and selected reaction monitoring (SRM) exhibit comparable linearity, dynamic range and precision for targeted quantitative HDL proteomics. J Proteomics. 2015;113:388-99. Epub 2014/12/03. doi: 10.1016/j.jprot.2014.10.017. PubMed PMID: 25449833; PubMed Central PMCID: PMCPMC4259393.
19. Manson JE, Chlebowski RT, Stefanick ML, Aragaki AK, Rossouw JE, Prentice RL, et al. Menopausal hormone therapy and health outcomes during the intervention and extended poststopping phases of the Women's Health Initiative randomized trials. JAMA. 2013;310(13):1353-68. Epub 2013/10/03. doi: 10.1001/jama.2013.278040. PubMed PMID: 24084921; PubMed Central PMCID: PMCPMC3963523.
20. Cagnacci A, Venier M. The controversial history of hormone replacement therapy. Medicina. 2019;55(9):602. doi: 10.3390/medicina55090602.
21. Raglan O, Kalliala I, Markozannes G, Cividini S, Gunter MJ, Nautiyal J, et al. Risk factors for endometrial cancer: An umbrella review of the literature. International Journal of Cancer. 2019;145(7):1719-30. doi: 10.1002/ijc.31961.
22. Grady D, Gebretsadik T, Kerlikowske K, Ernster V, Petitti D. Hormone replacement therapy and endometrial cancer risk: A meta-analysis. Obstetrics & Gynecology. 1995;85(2):304-13. doi: 10.1016/0029-7844(94)00383-o.
23. Azam S, Lange T, Huynh S, Aro AR, Von Euler-Chelpin M, Vejborg I, et al. Hormone replacement therapy, mammographic density, and breast cancer risk: a cohort study. Cancer Causes & Control. 2018;29(6):495-505. doi: 10.1007/s10552-018-1033-0.
24. Lacey JV, Jr., Brinton LA, Lubin JH, Sherman ME, Schatzkin A, Schairer C. Endometrial carcinoma risks among menopausal estrogen plus progestin and unopposed estrogen users in a cohort of postmenopausal women. Cancer Epidemiol Biomarkers Prev. 2005;14(7):1724-31. Epub 2005/07/21. doi: 10.1158/1055-9965.EPI-05-0111. PubMed PMID: 16030108.
25. Howlader N NA, Krapcho M, Neyman N, Aminou R, Waldron W, Altekruse SF, Kosary CL, Ruhl J, Tatalovich Z, Cho H, Mariotto A, Eisner MP, Lewis DR, Chen HS, Feuer EJ, Cronin KA, Edwards BK. SEER Cancer Statistics Review, 1975-2008. National Cancer Institute. 2010.
26. Sundar S, Balega J, Crosbie E, Drake A, Edmondson R, Fotopoulou C, et al. BGCS uterine cancer guidelines: Recommendations for practice. Eur J Obstet Gynecol Reprod Biol. 2017;213:71-97. Epub 2017/04/25. doi: 10.1016/j.ejogrb.2017.04.015. PubMed PMID: 28437632.
27. Wilczynski M, Danielska J, Wilczynski J. An update of the classical Bokhman's dualistic model of endometrial cancer. Prz Menopauzalny. 2016;15(2):63-8. Epub 2016/09/02. doi: 10.5114/pm.2016.61186. PubMed PMID: 27582678; PubMed Central PMCID: PMCPMC4993978.

28. Njoku K, Chiasserini D, Whetton AD, Crosbie EJ. Proteomic biomarkers for the detection of endometrial cancer. Cancers (Basel). 2019;11(10):1572. Epub 2019/10/19. doi: 10.3390/cancers11101572. PubMed PMID: 31623106; PubMed Central PMCID: PMCPMC6826703.
29. Ellenbroek B, Youn J. Rodent models in neuroscience research: is it a rat race? Dis Model Mech. 2016;9(10):1079-87. Epub 2016/10/14. doi: 10.1242/dmm.026120. PubMed PMID: 27736744; PubMed Central PMCID: PMCPMC5087838.
30. Iannaccone PM, Jacob HJ. Rats! Dis Model Mech. 2009;2(5-6):206-10. Epub 2009/05/02. doi: 10.1242/dmm.002733. PubMed PMID: 19407324; PubMed Central PMCID: PMCPMC2675817.
31. Bryda EC. The mighty mouse: The impact of rodents on advances in biomedical research. Mo Med. 2013;110(3):207-11.
32. Lemini C, Jaimez R, Figueroa A, Martinez-Mota L, Avila ME, Medina M. Ovariectomy differential influence on some hemostatic markers of mice and rats. Exp Anim. 2015;64(1):81-9. Epub 2014/10/15. doi: 10.1538/expanim.14-0052. PubMed PMID: 25312504; PubMed Central PMCID: PMCPMC4329519.
33. Owens JW, Ashby J. Critical review and evaluation of the uterotrophic bioassay for the identification of possible estrogen agonists and antagonists: in support of the validation of the OECD uterotrophic protocols for the laboratory rodent. Organisation for Economic Co-operation and Development. Crit Rev Toxicol. 2002;32(6):445-520. Epub 2002/12/19. doi: 10.1080/20024091064291. PubMed PMID: 12487363.
34. Shi R, Kumar C, Zougman A, Zhang Y, Podtelejnikov A, Cox J, et al. Analysis of the mouse liver proteome using advanced mass spectrometry. J Proteome Res. 2007;6(8):2963-72. Epub 2007/07/05. doi: 10.1021/pr0605668. PubMed PMID: 17608399.
35. Choi H, Fermin D, Nesvizhskii AI. Significance analysis of spectral count data in label-free shotgun proteomics. Mol Cell Proteomics. 2008;7(12):2373-85. Epub 2008/07/23. doi: 10.1074/mcp.M800203-MCP200. PubMed PMID: 18644780; PubMed Central PMCID: PMCPMC2596341.
36. Smith R, Tostengard AR. Quantitative evaluation of ion chromatogram extraction algorithms. J Proteome Res. 2020;19(5):1953-64. Epub 2020/03/29. doi: 10.1021/acs.jproteome.9b00768. PubMed PMID: 32216286.
37. Tabolacci C, De Martino A, Mischiati C, Feriotto G, Beninati S. The role of tissue transglutaminase in cancer cell initiation, survival and progression. Med Sci (Basel). 2019;7(2):19. Epub 2019/01/30. doi: 10.3390/medsci7020019. PubMed PMID: 30691081; PubMed Central PMCID: PMCPMC6409630.
38. Ishiwata T, Cho K, Kawahara K, Yamamoto T, Fujiwara Y, Uchida E, et al. Role of lumican in cancer cells and adjacent stromal tissues in human pancreatic cancer. Oncol Rep. 2007;18(3):537-43. Epub 2007/08/03. doi: 10.3892/or.18.3.537. PubMed PMID: 17671699.
39. Prokai L, Rahlouni F, Zaman K, Nguyen V, Prokai-Tatrai K. Proteomics complementation of the rat uterotrophic assay for estrogenic endocrine disruptors: A roadmap of advancing high resolution mass spectrometry-based shotgun survey to targeted biomarker quantifications. Int J Mol Sci. 2021;22(4):1686. Epub 2021/02/12. doi: 10.3390/ijms22041686. PubMed PMID: 33567512; PubMed Central PMCID: PMCPMC7914934.